The Thermal Conductivity of Metals at Low Temperatures

H. M. Rosenberg

Phil. Trans. R. Soc. Lond. A 1955 **247**, 441-497
doi: 10.1098/rsta.1955.0003

THE THERMAL CONDUCTIVITY OF METALS AT LOW TEMPERATURES

By H. M. ROSENBERG
The Clarendon Laboratory, University of Oxford

(*Communicated by K. Mendelssohn, F.R.S.—Received* 3 *August* 1954—
Read 3 *February* 1955)

CONTENTS

The thermal conductivity of high-purity samples of thirty-two metals has been measured. These were Ag, Al, Au, Be, Cb, Cd, Ce, Co, Cu, Fe, Ga, In, Ir, La, Mg, Mn, Mo, Ni, Pb, Pd, Pt, Rh, Sb, Sn, Ta, Ti, Tl, U, V, W, Zn and Zr. For most metals measurements were taken from 2 to 40°K, but where necessary they were extended to 90°K. For superconductors they were taken in both the superconducting and normal states. The conductivity was found to be entirely electronic except for Sb and U. Most of the specimens were polycrystalline, but single crystals of Zn, Cd, Sn, Pb, Ga and Ti were measured. For Zn and Ga, specimens of different orientations with respect to the rod axis were obtained, and in both these metals the thermal conductivity was found to be anisotropic. The thermal resistance, W, at low temperatures of nearly all the metals is of the form $W=\alpha T^2+\beta/T$, and the constants α and β have been calculated. If K_∞ is the limiting thermal conductivity at high temperatures and θ is the Debye temperature, then the value of $\alpha K_\infty \theta^2$ is the same for the metals in any one chemical group. For some metals the electrical resistance was measured at the same time as the thermal conductivity over the full temperature range and hence the Lorenz number, L, was calculated. The limiting value of L at low temperatures for several metals was found to be considerably higher than the theoretical value, in particular for Ti and Zr. A corresponding effect to the minimum in the electrical resistance of Mg has been found in the thermal resistance. A large increase in the thermal conductivity of Fe after a period of time has been ascribed to the precipitation of impurities in the metal. A method is given for estimating the thermal conductivity of a metal at low temperatures.

[Published 24 March 1955

1. Introduction

Until recently the main data on the thermal conductivity of metals at low temperatures dealt with superconductors and the change in conductivity during the normal-superconducting transition. Very little information had been obtained on the thermal conductivity of non-superconductors or of superconductors above their transition temperature. The existing results indicated that there was considerable disagreement with theory and that much more information would be required in order to gain a fuller understanding of the subject. It was for this reason that the investigations to be described in this paper were carried out. The main object has been the systematic collection of data so that a general picture of the heat conductivity of metals at low temperatures could be obtained. This seemed necessary in view of the present unsatisfactory state of the theory, for which the results may be of use in pointing the way to the theoretical modifications which are needed. Besides this, the technical information which they yield is itself of importance in many cases. Because of the disagreement between theory and experiment, a detailed analysis of the results is rather unprofitable and has not been attempted. Electrical resistance measurements were also taken on many of the specimens so that the variation of the Wiedemann–Franz relation could be studied.

The work to be described has been concerned with the measurement of the thermal conductivity of as many metals as could be obtained in an extremely pure state, i.e. a purity greater than 99·9 %. The conductivity of a metal which is less pure than this will be reduced and will be dictated almost entirely by the amount of impurity present, and the results will be of little use in determining the properties of the metal itself. Hence the need for very pure samples. Thirty-two metals have been measured, most of them over the temperature range 2 to 40° K (or, where it seemed of interest, up to 90° K). In some cases two or more samples of the same metal have been used. For superconductors with transition temperatures above 2° K, readings were taken in the superconducting state and in a magnetic field sufficient to destroy the superconductivity. The effect of high magnetic fields on the thermal conductivity of metals in the normal state was also investigated, but this has been reported separately (Mendelssohn & Rosenberg 1953).

The first sections of this paper deal with the apparatus and the experimental technique used. Next follows an outline of the present state of the theory and the results of the experiments. Finally, these results are discussed with reference to the theoretical predictions and a method of estimating the thermal conductivity of a metal sample is suggested.

2. Experimental arrangement

The general experimental arrangement is shown in figure 1. The thermal conductivity measurements were made on specimens in the form of rods which were about 5 cm long and 1 to 3 mm in diameter. Heat was applied at one end of the specimen *S*, by a small electric heater, *H*, which had a resistance of about 100Ω. This heater was made of 47-gauge eureka wire which was wound on to the specimen and stuck to it with celluloid cement. The other end of the specimen was kept cold by anchoring it to a thick copper rod, *R*, which was in turn in good thermal contact with the high-pressure chamber, *P*, of a Simon expansion liquefier. This type of liquefier is exceedingly useful for this work (Mendelssohn

& Pontius 1937; Olsen 1952), as it can be used to cover a continuous temperature range from 2 to 90° K. The method for doing this will be described in this and the next section. The temperature difference produced by a given heat input was measured with two gas thermometers, T, which were attached by Wood's metal to copper contacts, C, spaced 3 cm apart along the specimen. These thermometers were connected to either side of a U-tube containing butyl phthalate (see fig. 2) in order that the pressure difference and hence the temperature difference could be measured. A third tube, which was kept continuously pumped, was connected to the bottom of the U-tube, and this was used to measure the absolute pressure in the thermometers.

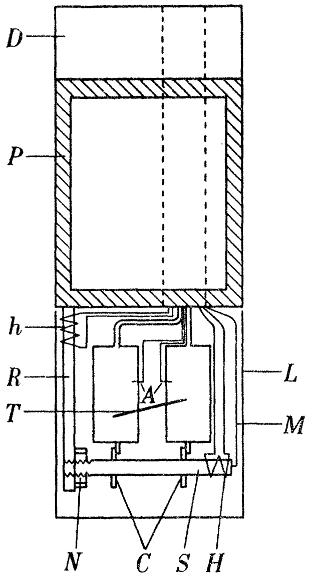

FIGURE 1

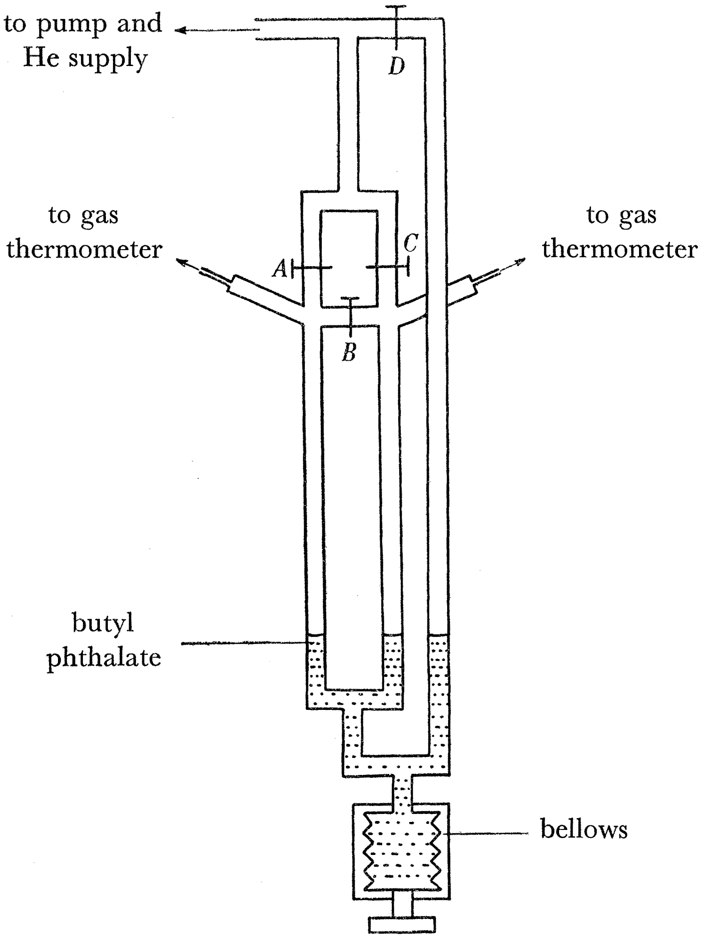

FIGURE 2

FIGURE 1. Diagram of the apparatus used for the thermal conductivity measurements. S is the specimen, H is the heater which produces the temperature gradient measured by the two gas thermometers T. The other end of the specimen is kept cold by being connected to the helium container P by the thick copper rod R. Copper contacts C join the specimen to the thermometers. M was the current lead, and A were the potential leads which were used to measure the electrical resistance of the specimen.

FIGURE 2. The manometer system used to measure the gas-thermometer pressures. The bellows enabled the thermometers to be operated under constant-volume conditions.

Current and potential leads were attached to the heater so that the heat input could be calculated. The potential was measured on a Clark Fisher potentiometer, and this was also used to measure the heating current by passing it through a 100 Ω standard resistance and observing the potential produced.

In order that as many specimens as possible could be measured in a reasonably short time, it was essential to have an arrangement whereby a new specimen could be fitted into the apparatus with as little delay as possible. For this reason the samples were made with a 2 B.A. thread cut at the cold end, and this was screwed into a corresponding hole tapped into the end of the copper rod which connected to the liquid-helium chamber. To ensure good thermal contact this hole was tapped under size, and whenever possible the contact was improved by running soft solder or Wood's metal through the screw joint. If the specimen was too small to enable a 2 B.A. thread to be cut on it, then it was soldered or screwed into a copper bush which had a 2 B.A. thread cut on the outside. To facilitate mounting the specimen, a 2 B.A. brass nut, *N*, was soldered to the thread about half a centimetre from the end (see figure 1). A small spanner could then be used to fit or remove the specimen without any undue strain being imposed on it. The specimen was mounted horizontally. The reason for this was that when measurements in a magnetic field were taken, the same iron-cored magnet could be used for the application of both transverse and longitudinal fields.

The copper contacts, *C*, to which the gas thermometers were soldered were usually in the form of thin disks with a hole in the centre through which the specimen passed. These disks were generally soft-soldered to the specimen. For specimens with a low melting-point, Wood's metal was used. Others which would not solder had to be brazed. Another method used, when soldering was not possible, was to spot-weld a small platinum ring (made by flattening some platinum wire) around the specimen and then to solder the copper disk to this ring. This was used for the tantalum, niobium, titanium and zirconium specimens. For aluminium and magnesium, small copper clamps were fixed to the rod to provide thermal contact. The use of aluminium solder did not prove satisfactory for this purpose. For some of the more delicate specimens an annealed copper wire was wound round the rod and soldered to it. In the case of gallium, which melts at 30° C, a copper wire was heated gently and was pushed into the rod which melted at the point of contact. When the gallium had solidified again it made a strong connexion. The other end of this wire was attached to the gas thermometer by a small clamp and celluloid cement, as no heat could be applied for soldering. In all cases the thermal contacts were made 3 cm apart along the specimen, so that once they had been arranged, the gas thermometers were always in the correct position for attachment. Because of this standard set-up a specimen could be changed in an hour or two.

The specimen and the gas thermometers were surrounded by a copper radiation shield, *L*, which was always kept at roughly the temperature of the specimen since it was fitted to the helium container. Around this shield and the helium liquefier was a brass vacuum jacket which thermally isolated the whole of the interior of the apparatus.

The gas thermometer system was designed to have as small an external volume as possible. The thermometers themselves were copper cylinders, each of which had a volume of approximately 3 cm^3. They were connected to the manometer system by stainless steel capillaries which had an inside diameter of 0·8 mm. To prevent heat influx to the specimen along these capillaries, they were anchored both to the top of the liquefier and also to the vacuum jacket. The manometer was made of 1 mm bore precision capillary glass tubing, and the total dead volume was only about 1 cm^3. Because this was so small the corrections to the temperature measurements were not very large, being very much less than 1 %. To achieve such a small dead volume it was not possible to have any oil traps between the manometer and the metal capillary tubing, and great care had to be taken that the oil did not rise too high in the manometer. It was found that the safest procedure was to keep all the manometer taps open so that no pressure differences could be created in the system and to close them only when the apparatus had reached liquid-hydrogen temperature. Before allowing the apparatus to warm up after an experiment they were all opened again. If oil does get into the gas thermometers they must be changed because helium gas is adsorbed by the oil, giving rise to incorrect temperature readings.

The manometer system is shown in figure 2. The brass bellows at the bottom are used to adjust the oil levels so that the thermometers may be used under constant-volume conditions. When a temperature difference was present, the pressures in the two thermometers, and hence the levels in the U-tube, were different, and so only one thermometer could be kept at constant volume throughout the experiment. In general, however, the pressure difference was sufficiently small to enable the volume of the other thermometer to be assumed constant as well. A scale was fixed behind the manometer and the levels were viewed with a telescope. This enabled them to be measured to 0·1 mm with ease.

In order that measurements could be taken above the boiling-point of liquid hydrogen, a heater with a resistance of about 200 Ω was wound around the copper bar to which the specimen was attached. This is shown as *h* in figure 1. By applying voltages of up to about 12 V across this heater the temperature of the apparatus could be raised to 40° K or slightly higher. In some cases it was advisable to take readings above 40° K. These temperatures were achieved by condensing liquid oxygen into the helium container and allowing this oxygen to evaporate under reduced pressure. In this way readings could be made between 55 and 90° K.

In some of the later work a much more convenient method for covering the range 20 to 90° K was used. The apparatus was cooled to 90° K and the thermometers were filled and calibrated at this temperature. The high-pressure chamber was then filled with helium at a pressure of about 100 atm. Exchange gas was pumped out of the vacuum system and the Dewar surrounding the apparatus was removed, and the liquid oxygen in it emptied. The Dewar was then replaced and filled with liquid hydrogen. A small amount of exchange gas was let into the vacuum space so that the liquid hydrogen would start to cool the apparatus to the first temperature at which an experimental point was required (say 80° K). When this temperature had been reached (as indicated by the gas thermometers) the exchange gas was pumped out. The thermal capacity of the high-pressure helium was sufficient to keep the temperature constant to a few tenths of a degree while a thermal conductivity point was being taken. When this had been done, exchange gas was let in again and the apparatus was cooled down to the temperature at which the next point was required. This process was repeated right down to 20° K, and it was found to be a most satisfactory method for covering this temperature range.

Temperatures in the range 10 to 20° K were attained as part of the normal helium liquefaction process by pumping the liquid hydrogen which is contained in a small copper can attached to the high-pressure helium chamber. By controlling the pumping rate the apparatus could be held at any temperature in this region.

For readings below 4·2° K the helium in the chamber was pumped and temperatures of about 1·4° K could be achieved. No readings were taken as low as this, however, since the pressure in the gas thermometers at any temperature must always be less than the saturated vapour pressure of the helium at that temperature. This necessitates a very low pressure (a few centimetres of oil) in the gas thermometers at 1·4° K, with a consequent loss in accuracy. In a few cases the thermometers were used as vapour-pressure thermometers at the lower temperatures, but this was not very successful, probably due to film flow up the capillaries. In most cases readings were not taken below 2·0° K.

Temperatures between the lowest point to which hydrogen could be pumped (about 10° K) and the boiling-point of liquid helium (4·2° K) were obtained by controlling the expansion of the high-pressure helium through a needle valve (MacDonald & Mendelssohn 1950). Instead of expanding the helium at 10° K from a pressure of 120 atm directly to atmospheric pressure at 4·2° K, it was allowed to expand more slowly, and by careful control any temperature above 4·2° K could be held constant. In this way the expansion could be made to last for between 1 and 2 h, several points being taken during this time. While this procedure did limit the yield of liquid helium, it was found that the liquid still lasted till about 6 h from the beginning of the expansion.

3. Experimental procedure

Before beginning an experiment the gas thermometers and manometer system were pumped out for about an hour, all the taps shown in figure 2 being left open. This pumping was continued while the apparatus was cooled to liquid-hydrogen temperature. The tap *D* was then closed and clean helium was introduced through the pumping line to fill the thermometers via *A* and *C*. During this time the bellows were adjusted to keep the oil levels within the U-tube, and this forced oil up the extreme right-hand tube which was still evacuated. The filling was continued until the oil had been forced nearly to the top of this tube. This ensured a pressure of about 50 cm of oil in the thermometers. The taps *A*, *B* and *C* were then closed and *D* was opened and kept pumped. The apparatus was left until the pressure in the gas thermometers reached a constant value, the oil in the U-tube always being adjusted by the bellows to a fixed mark. This pressure was recorded as the thermometer calibration at the temperature of liquid hydrogen boiling under atmospheric pressure.

The interior of the apparatus was then pumped free of helium exchange gas so that the specimen was thermally isolated from the bath of liquid hydrogen. The pressure achieved was of the order of 10^{-5} cm of mercury. A current was then passed through the heater attached to the specimen. This caused a temperature difference to be set up along the specimen and thus a difference of levels was indicated in the U-tube. The heating current was adjusted so that the difference in the oil levels was about 1 cm. The current required was usually a few milliamperes. The levels were viewed through a telescope, the lower level being kept on the fixed mark by adjusting the bellows. After equilibrium was established, which usually took about 5 min, the difference in levels was noted to the nearest 0·1 mm. The oil level in the evacuated tube was also measured. The heating current and the potential across the heater were then recorded. This data enabled the thermal conductivity at 20° K to be calculated.

The can (*D* in figure 1) which was fixed on to the helium container was then filled with liquid hydrogen, and this was pumped until it and the rest of the apparatus had reached a temperature of about 17° K. The pump was then throttled until the temperature of the apparatus remained constant, although usually the heat leak was so small that the pump could be closed off completely and the temperature of the apparatus remained steady. The oil levels in the U-tube were adjusted to the fixed mark and they were checked to see that they were equal. The heating current was then turned on and a further determination of the thermal conductivity was made. The hydrogen was then pumped to 14 and 11° K, where more points were taken. If the results indicated a rapid change of conductivity in this region, then, of course, readings were taken at smaller temperature intervals.

Owing to the fact that the volumes of the gas thermometers were not exactly equal, the oil levels in the U-tube were not exactly the same at the lower temperatures even before the heating current was applied. This difference in levels was only a few tenths of a millimetre, and it was subtracted from the measurements obtained when the current was on.

After the reading at 11° K the hydrogen was pumped vigorously for about an hour and a half when a temperature of 9·6 to 10° K could be achieved. This temperature being about one-half the filling temperature of the thermometers, their pressure had now fallen to half the filling pressure. More gas was therefore put into the thermometers until the pressure in them was again 50 cm of oil. The pressures in the thermometers were equalized by opening tap *B* for a few minutes. By refilling in this way, the sensitivity of the thermometers was increased. A given current would now give twice the pressure change it did previously and, conversely, smaller currents could be used to give the same pressure change. Hence much smaller temperature differences could be used, and this was particularly important if the conductivity was changing rapidly.

After the thermometers had been refilled, a thermal conductivity point was taken at 9·6° K. The hydrogen pumping was then stopped and the helium was allowed to expand slowly, as has been described in §2, so that readings could be taken at intervals of about 1·5° down to 4·2° K, where the expansion to atmospheric pressure was completed. At liquid-helium temperature, time was allowed for the thermometers to become quite steady. Their pressure at this temperature was used as the calibration point for all the readings taken below 9·6° K, i.e. after the thermometers had been refilled.

Measurements of the thermal conductivity below 4·2° K were taken in a similar manner, the liquid helium being pumped to the required temperatures. Depending on the order of magnitude of the conductivity, the thermometers were sometimes filled again to a pressure of 50 cm of oil at 4·2° K. They were always checked against the vapour pressure of the helium at two or three temperatures below 4·2° K. In the liquid-helium region the equilibrium time was usually quite short, generally being of the order of a minute or two.

After the readings in the helium range had been completed, the thermometer taps were all opened and the apparatus was allowed to warm up to the temperature of liquid hydrogen by letting exchange gas into the vacuum jacket. The thermometers were then filled to about half their maximum pressure and a calibration point was taken. Readings up to about 40° K were then made by passing a current through the heater wound on the specimen support to raise the temperature of the specimen to the value required. The presence of liquid hydrogen in the can attached to the helium container greatly assisted the attainment of a temperature equilibrium in this region. At these higher temperatures the equilibrium time increased greatly and could be as much as 20 min in some cases.

This was the procedure used to obtain measurements of the conductivity in the range 2 to 40° K. It was usually possible to do a complete run on a specimen in about 14 h, and thus a large number of specimens could be investigated. The results on some specimens indicated that readings above 40° K would be of interest and measurements between 40 and 90° K were taken separately. The general method of taking readings above 40° K has already been mentioned. The procedure was similar to that in the range 10 to 20° K, except that the thermometers were filled and calibrated at 90° K, the temperature of liquid oxygen at atmospheric pressure.

3·1. *The form factor*

For each specimen the form factor, F, had to be measured, where F is the ratio of distance between thermometer contacts to mean cross-section of specimen. In general the determination of F presented little difficulty, since the specimens usually had a circular or rectangular cross-section. For specimens which did not have a regular cross-section, such as single crystals, the mean area of cross-section was found by weighing it and measuring its overall length. A knowledge of the density, from standard tables, enabled the area to be calculated. Since even these specimens had a fairly uniform cross-section throughout their length, this method was quite satisfactory.

Another method of measuring F was adopted for the lanthanum specimen which was very short (about 1 cm) and had a comparatively large, square cross-section. Although in this instance the dimensions could be measured fairly easily, it was exceedingly unlikely that the flow lines would be parallel to the length of the specimen over most of its length, and so the effective value of F might be considerably different from that calculated. A copy of the lanthanum specimen was made in stainless steel, the electrical resistivity of which at room temperature was accurately known. The electrical resistance of this piece of steel, whose connexions were of the same form and in the same place as those on the lanthanum, was measured, and hence its form factor could be calculated. In most of the other specimens the diameter was less than 5 % of the length, and the size of the thermometer contacts themselves was also small ($\sim$2 %) compared with the length between the thermometers. Thus the flow lines could be assumed to be parallel to the length of the specimen in all these cases.

4. CALCULATION OF RESULTS

The thermal conductivity, K, can be calculated from the equation

$$K = \frac{\dot{Q}F}{\Delta T},$$

where $\dot{Q}$ is the heat passing per second along the specimen, ΔT is the temperature difference it produces and F is the form factor. $\dot{Q}$ can be obtained directly from the current and potential measurements. F may be calculated from the dimensions of the specimen, as has been described in § 3·1. The only quantity left to calculate is ΔT. This is done from the gas thermometer pressures assuming the validity of the ideal gas equation, $PV/T=$ constant.

Since the calculation is quite straightforward only the relations used will be quoted. If p_1 and p_2 are the pressures in the two thermometers corresponding to temperatures T_1 and T_2 and T is the mean of T_1 and T_2, then

$$\begin{aligned}\Delta T = T_1 - T_2 &= 2T(p_1-p_2)/(p_1+p_2)\\ &= T(p_1-p_2)/p,\end{aligned} \tag{1}$$

where p is the mean of p_1 and p_2. Taking into account the external volume of the thermometers, T is calculated from the expression

$$T = pT_0/(p_0+E), \tag{2}$$

where T_0 and p_0 are the calibration temperature and pressure respectively and

$$E = (v/V)\ (T_0/T')\ (p_0-p), \tag{3}$$

v being the external volume of the thermometer system, V the internal volume of the thermometers and T' the mean temperature of the external volume. It can be seen that the correction term E is very small since T' is approximately room temperature while T_0 is generally either 20 or 4° K; v/V was 0·27. Only when T_0 is 90° K does E become greater than 1 % of p. It will be noted that for a given calibration temperature, T_0, the value of E is of the form: constant $\times\ (p_0-p)$, and so it was quite simple to calculate E for any value of p.

For the temperatures and pressures used, corrections for thermomolecular effects and for the second virial coefficient are so small that they can be neglected. Heat losses by radiation, conduction along leads and thermometer capillaries and through the low-pressure gas in the cryostat where the specimen was mounted were all negligible.

We assume in these calculations that the volumes of both thermometers remain constant. While this is strictly true only for one of them, namely, the one whose oil level is always kept on the fixed mark, nevertheless the difference in oil levels is usually so small that the change in external volume is only about 1 %, and this does not affect the temperature calculation.

5. Accuracy of the experimental results

The main error in the determination of the thermal conductivity lies in the measurement of the temperature difference. The electrical measurement of the heat input usually involved less than 0·1 % error, and although the accuracy of the form factor was limited by the measurement of the distance between the thermometer contacts, thereby giving a possible error of 1 to 2 %, this stayed constant throughout the readings on one specimen and did not affect the relative values of the conductivity taken at different temperatures.

The temperature difference that was used was in general indicated by a pressure difference of about 1 cm of oil, and this could be measured to 0·1 mm with the telescope. If this is coupled with a possible 'zero' error in the oil level reading (i.e. before any heat is applied) an error of about 2 % might have occurred. Thus the relative error in a set of readings on one specimen might be ±2 %, and the absolute error in the thermal conductivity should not be more than ±3 %. The mean temperature of the specimen was in all cases accurate to 0·1° K and was generally much better than this in the liquid-helium region.

6. Measurement of the electrical resistance

The electrical resistance of most of the specimens was measured at room temperature (ρ_{293}) and at the temperature of liquid hydrogen (ρ_{20}). This was generally done after the specimen had been removed from the thermal conductivity apparatus. A current of about 0·5 A was passed through the specimen, and the potential produced across the copper contacts, with which the specimen had been attached to the thermometers, was measured on a galvanometer amplifier (MacDonald 1947). In this way the form factor used in the electrical measurements was the same as that used in the thermal ones. Even if there was a slight error in the absolute value of the form factor then this would not affect a comparison of thermal and electrical measurements.

The electrical measurements were useful as a guide to the purity of the specimens and also, as will be amplified later, they enabled the electronic heat conductivity to be calculated. Such calculated values are indicated on the thermal conductivity curves by a ringed point. The ratios ρ_{293}/ρ_{20} are given in table 1 (p. 457).

It was later found possible to make electrical measurements during the actual thermal conductivity experiment. The advantage of this is that no damage can occur to the specimen between thermal and electrical measurements and so the two can be more confidently compared. Even a slight amount of bending might affect the conductivities of a soft specimen. One current lead (M in figure 1) was fixed to the free end of the specimen just beyond the small heater and the framework of the liquefier was used as the other. One potential lead, A, was connected to each gas thermometer. While the gas thermometers themselves are connected to one another and to the rest of the apparatus by metal capillary tubing, the resistance between the two thermometers was about 2 Ω, whereas that of the specimen was of the order of $10^{-6}\,\Omega$ and so no short-circuiting of the measuring current occurred. The main difficulties arose from the fact that the specimen was mounted for a thermal conductivity experiment and was thermally isolated in a high vacuum. Thus when a current was passed through it for an electrical measurement an appreciable temperature gradient could be produced which might make it difficult to take such a measurement. Nevertheless, with care, measurements could be taken even to liquid-helium temperatures. These gave valuable data for comparison of electrical and thermal conductivities, particularly where, as with magnesium, anomalies were known to exist in the electrical conductivity. The arrangement was also very useful when fragile specimens were being measured, as an immediate indication was given if the specimen was damaged or broken.

7. The theory of the thermal conductivity of metals

The heat transport in a metal is usually considered as being due to the sum of transports arising from two separate mechanisms. First, there is the conduction of heat by the lattice, which also occurs in dielectrics, and secondly, there is the conductivity which is due to the transport of heat by the conduction electrons. It is found that in a dielectric the lattice conductivity can be quite considerable and is, in fact, of the same magnitude as the electronic conductivity in a metal. In a fairly pure metal, however, it is extremely small compared with the electronic contribution and it can nearly always be neglected. This is because the conduction electrons act as extremely efficient scatterers of the lattice waves and hence reduce their importance in the conduction process. For this reason we shall assume that the lattice conductivity is negligible, and we shall, in the main, only consider the transport of heat by the electrons.

The calculation of the thermal and electrical conductivities of a metal requires the solution of the Boltzmann equation in order to determine the velocity distribution function of the electrons under the influence of an external field or a temperature gradient. In general, the solution is very complicated and it has so far been carried out only for the simple case of quasi-free electrons where the energy, E, is of the form

$$E=\frac{h^2}{8\pi^2m^*}|\mathbf{k}|^2, \tag{4}$$

$\mathbf{k}$ is the wave vector, m^* is the effective mass of the electron and h is Planck's constant. It should be noted that by choosing a suitable value of m^* we can, in fact, take account of quite complicated potential distributions.

The solution of the problem has been considered by Wilson (1937), who has calculated a zero-order approximation applicable at low temperatures, and it has been dealt with in more detail by Makinson (1938), Kroll (1938), Kohler (1949), Sondheimer (1950), Umeda and his co-workers (Umeda & Toya 1949; Umeda & Yamamoto 1949, 1951) and Ziman (1954). The general form of all their results is the same and, except for Ziman's work, they have been considered together in a previous paper (Olsen & Rosenberg 1953). Briefly the results are as follows.

The thermal conductivity due to the transport of heat by the electrons will be limited by any processes which will tend to scatter the electrons. At low temperatures there appear to be two such processes. First, the scattering of the electrons by impurities in the metal. These can be either chemical impurities, e.g. foreign atoms, or physical impurities such as lattice defects. The second scattering process is that by which the thermal vibrations of the crystal lattice itself will tend to limit the mean free path of the electrons. Each of these processes can be considered to produce its own contribution to the thermal resistance, W, and these can be added to give the total resistance. The independence of these two scattering mechanisms is the basis of Matthiesen's rule, and Sondheimer (1950) has shown that while this is not strictly correct, the error involved in a simple summation of the two resistances is only of the order of 1 %.

On these considerations we therefore have

$$1/K=W=1/K_0+1/K_i=W_0+W_i, \tag{5}$$

where K is the total thermal conductivity of the metal, W the corresponding resistance, W_i and W_0 the individual resistances due to the impurities and the lattice vibrations respectively, and K_i and K_0 the corresponding conductivities.

W_i can be dealt with fairly simply. We can use the general result from kinetic theory that K_i is proportional to cvl, where c is the specific heat per unit volume, v is the velocity and l the mean free path of the electrons. The impurities in the metal will limit l. This will not depend on temperature and so we can consider it constant. If we also assume that v is constant then K_i is proportional to c. Since, for electrons, c is proportional to T it follows that K is proportional to T or W_i is proportional to $1/T$.

K_i is connected with the residual electrical conductivity, σ_i, of a metal by the Wiedemann–Franz law

$$\frac{K_i}{\sigma_i T} = L_0, \text{ a constant, called the Lorenz number,} \tag{6}$$

where
$$L_0 = \frac{\pi^2 k^2}{3\epsilon^2} = 2{\cdot}45 \times 10^{-8}\,\mathrm{W}\Omega/\mathrm{deg}^2, \tag{7}$$

k being Boltzmann's constant and ϵ the electronic charge. It can be seen that since σ_i is constant we should again expect K_i to be proportional to T, as we saw in the simplified argument of the previous paragraph. This relation holds very well in most cases, even to the numerical value of L_0.

The solution of the lattice scattering term, W_0, is much more complicated as the Wiedemann–Franz law does not hold in this case. It is, however, more important from a fundamental viewpoint than is W_i, since W_i will vary from one sample to the other of the same metal, whereas W_0 should have the same value for any reasonably pure sample of a given metal. From a qualitative point of view one can see the general form of the temperature dependence of W_0. As the temperature is decreased the energy of the lattice vibrations becomes less and so one would expect them to scatter the electrons to a smaller extent, i.e. W_0 should decrease with temperature. In actual fact, the theory predicts that W_0 is proportional to T^2 below $T = \theta/10$, where θ is the Debye temperature. The constant of proportionality, α, is given by

$$\alpha = \frac{G N_a^{\frac{2}{3}}}{K_\infty \theta^2}; \tag{8}$$

G is a numerical factor equal to 95·3 in Makinson's and Wilson's work, and is equal to 72 in the more exact solution by Sondheimer; N_a is the number of conduction electrons per atom; and K_∞ is the limiting thermal conductivity at high temperatures.

Thus the total thermal resistance of a metal at low temperatures is of the form

$$W = W_0 + W_i = \alpha T^2 + \beta/T, \tag{9}$$

where α is given by equation (8) and $\beta = 1/(\sigma_i L_0)$. It can be seen that provided W_i is not too large, we should get a minimum in the thermal resistance at low temperatures, i.e. a maximum in the thermal conductivity. The smaller the term W_i, that is, the purer the sample of a given metal, the lower the temperature of this maximum. A large value of α would also shift the maximum to lower temperatures, and this might occur if θ was small.

A graph of the temperature dependence of the thermal conductivity as calculated by Sondheimer for a monovalent metal with various impurity contents is shown in figure 3. The impurity parameter, P, in this figure can be calculated from

$$P = \frac{\rho_i}{\rho_T}\left(\frac{T}{4\theta}\right), \tag{10}$$

where ρ_i is the residual electrical resistance and ρ_T is the electrical resistance at a temperature T, high enough for $(\theta/T)^2$ to be small compared with unity. The ordinate of the graph represents the conductivity, K, multiplied by the factor $12A/(\pi^2 L_0 \theta)$, where

$$A = \rho_T \theta / T. \tag{11}$$

The linear section of the curve at low temperatures as well as the maximum are clearly indicated. Another general feature of the solution is the existence of a minimum in the conductivity at about $\theta/5$, providing the metal is not too impure, above which temperature the conductivity rises slowly to a constant value at high temperatures.

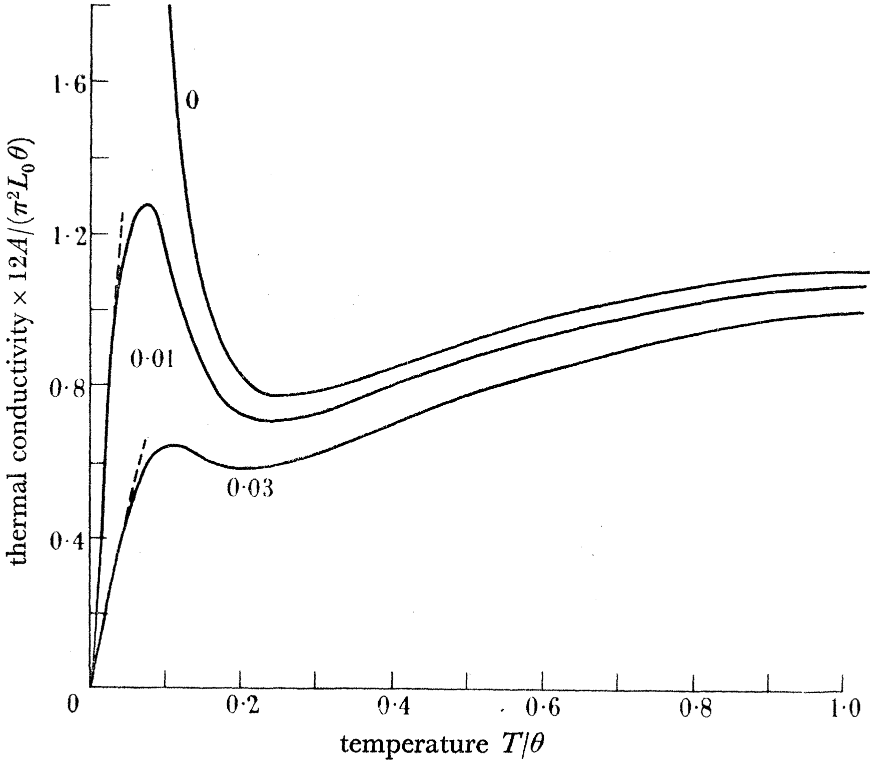

FIGURE 3. The thermal conductivity of a monovalent metal as calculated by Sondheimer for different values of the impurity parameter, P, indicated on the curves.

It should be emphasized that the Wiedemann–Franz law holds at low temperatures only for that part of the thermal resistance which is dictated by impurity scattering. It does not hold as a relation between the temperature-dependent electrical resistance and the thermal resistance due to lattice vibrations, W_0. The reason for this is that at low temperatures there will be present only lattice waves of low energy. These will scatter the electrons through small angles and so the general electron current drift will not be greatly affected. Nevertheless, at these collisions the electron can still lose energy of the order of kT and this will give an appreciable thermal resistance. Thus in this region the thermal resistance decreases less rapidly than the electrical resistance and hence the value of the Lorenz number falls below L_0. In the impurity resistance region, at still lower temperatures, the scattering is once more perfectly random and is equally efficient for both the electrical and the thermal resistance. Hence the Lorenz number in this region has the value L_0 once more. Therefore, if we calculate the Lorenz number L, using the total thermal and electrical conductivities we shall obtain the theoretical value L_0 as given in equation (7) only if we are in the region where W_i and $1/\sigma_i$ are the dominant terms. Above this temperature the value of L decreases and Makinson (1938) gives a graph showing that there should be minimum in L, the position of this minimum depending on the purity of the specimen. Above this minimum the value of L rises gradually to L_0 again.

The lattice conductivity

In some cases, if the metal is very impure, or if for some other reason it has a high impurity resistance, W_i, the electronic thermal conductivity might be so reduced as to make it comparable with the lattice conductivity, K_g. This can be detected by measuring the electrical and thermal conductivities of the specimen and then calculating the Lorenz number, L, where

$$L = \frac{K}{\sigma T}. \tag{12}$$

If this comes out to be higher than the theoretical value L_0, as defined by equation (7), then there is a likelihood of an appreciable lattice conductivity since L_0 will only be obtained if the electronic thermal conductivity K_e is used in the calculation and not the total thermal conductivity. By using the experimental value of σ in equation (12) and equating it to L_0, K_e may be calculated. Hence, since the total K has been measured, the value of K_g can be found.

In a metal, K_g is limited at low temperatures by the scattering of the lattice waves by the electrons. This has been shown (Makinson 1938) to give a conductivity proportional to T^2. Such an effect is shown by the antimony specimen (§8·9).

Comparison of the theory with experiment

Qualitatively the agreement between experimental results and the curves calculated from theory is quite satisfactory. In general the graphs of conductivity against temperature are similar to those shown in figure 3. At the lowest temperatures the conductivity increases and then, as W_0 becomes dominant, the conductivity increases less rapidly and has a maximum in the region of $\theta/10$ for high-purity specimens. Beyond this maximum, however, the conductivity decreases monotonically as the temperature is increased. No sign of a minimum has, as yet, been observed (except for a very shallow one in tantalum, §8·8), although it has been carefully looked for both in the present investigations and in previous work (e.g. Berman & MacDonald 1951). It should be pointed out, however, that the simpler solution of Makinson (1938) only gives a minimum in the conductivity if N_a in equation (8) is greater than about 0·3, whereas, as will be seen below, if experimental values of α are put in that equation, N_a comes out to be very much less than this. Therefore it is not really surprising that the pronounced minimum in the conductivity has not been observed.

From equation (9) it can be seen that a graph of WT against T^3 should be a straight line where the equation holds; i.e. below about $\theta/10$. The slope of this line should be α, and the intercept on the WT axis should be β. In practice such a straight line is obtained and hence α and β may be calculated. It is found that α is approximately the same for any sample of a given metal, which is what the theory leads one to expect. Using these values of α, N_a can be calculated from equation (8). It is then found that N_a comes out to be about

0·02 electron/atom (Hulm 1950) for a large number of metals, whereas the number of free electrons is generally thought to be of the order of one per atom. If this low value of N_a had any real significance we would also expect an appreciable lattice conductivity in monovalent metals and there is no evidence of this.

A possible difficulty in the calculation of N_a has been suggested by Blackman (1951), who states that since to a first approximation the Bloch theory only allows interactions between the electrons and the longitudinal lattice vibrations, a different θ, θ_L, should be used instead of the specific heat θ, when N_a is calculated. Blackman has calculated some values of θ_L, and these do give larger values of N_a. If, however, θ_L were the correct θ to use we should expect an appreciable lattice conductivity to be present due to the transverse waves which would not then be scattered by the electrons. Such an extra conductivity has not been observed.

Sondheimer (1952*a*, *b*) has pointed out that the Wilson–Makinson theory is in any case invalid if the number of free electrons per atom, N_a, is small. He shows that for N_a less than $\frac{1}{4}$, the usual expressions have to be modified and there is in fact a minimum value for α. This minimum value is still higher than those found experimentally, and the only way to lower the theoretical values of α so that they include those found by experiment is to consider either or both of N_a and θ to be arbitrary parameters and to adjust them as required. Sondheimer considers that this might be justifiable in view of the greatly simplified model of a metal which has been adopted.

Klemens (1954) has suggested that the form of the trial function which Sondheimer has used in this solution of the integral equation may not be the correct one to use. Klemens has solved the integral equation by two different methods, and he obtained as the coefficient G in equation (8) the value 64. This does improve the situation to some extent, but still not enough to consider the solution a satisfactory one.

An important contribution to the solution of the problem has been made recently by Ziman (1954). He has taken into account the fact first shown by Peierls (1929) that when an electron is scattered by a lattice vibration (phonon) two types of mechanism are possible depending on the values of the wave vectors **k** and **p** of the electron and phonon respectively. In both these processes energy is conserved but they differ in the momentum conditions. In one process momentum is conserved, i.e. if **k** and **k′** are the wave vectors of the electron before and after a collision with a phonon, respectively, then

$$\mathbf{k}' = \mathbf{k} + \mathbf{p}. \tag{13}$$

This type of scattering is the only one that has been considered by Wilson and all the other workers who have been mentioned above.

There is, however, another type of scattering that can occur. This is the so-called umklapp process or U-process, in which the initial total wave vector differs from the final total wave vector by a vector parallel to one of the principal axes of the reciprocal lattice. Thus in this process momentum is not conserved in the phonon system, but part of it is transferred to the lattice as a whole. If $\mathbf{g}_0$ is a basic vector of the reciprocal lattice then, for a U-process

$$\mathbf{k}' = \mathbf{k} + \mathbf{p} + \mathbf{g}_0. \tag{14}$$

Peierls has considered U-processes in connexion with the thermal conductivity of dielectrics (see Berman 1953), and he has shown that except at very low temperatures they are the main cause of thermal resistance. Since $\mathbf{g}_0$ is of the same order of magnitude as the maximum phonon wave number, it can be seen from equation (14) that $\mathbf{k}'$ can differ considerably from $\mathbf{k}$ and that a *U*-process can scatter an electron much more effectively than can the more orthodox case of equation (13). Hence they should be taken into account in any theory of conductivity.

Bardeen (1937) has considered the influence of *U*-processes in connexion with the electrical resistance of metals. This work has been developed by Ziman who has investigated the temperature variation of both the thermal and electrical resistances. The most interesting point in his solution is that at intermediate temperatures, where the *U*-processes become more numerous, the minimum in the thermal conductivity curve is almost entirely removed. Thus one of the problems of the theory now appears to be solved. Quantitatively, his solution is in very good agreement with the measurements on sodium by Berman & MacDonald (1951).

The above brief outline of the theory shows that when considered in detail, there are considerable discrepancies if it is compared with experimental results. Nevertheless, it should be noted that the general form of the conductivity curves for the monovalent metals is given satisfactorily. For metals of higher valency the main results of the theory agree qualitatively with experiment, even though one might have thought that the situation had been so over-simplified that no useful correlation could have been achieved.

8. Experimental results

8·1. *Introduction*

A general review of previous work in this field has already been given (Olsen & Rosenberg 1953), and the present results will be compared with those of other workers when the individual metals are discussed. The amount of systematic work that has been done in thermal conductivity measurements, has not, however, been very great and in most cases the temperature range has been restricted, having covered either the liquid-helium region or else that above 20° K. Usually only isolated metals have been measured. It seemed very desirable, therefore, to start an investigation in which the thermal conductivities of as many metals as could be obtained in an extremely pure state were measured over a wider temperature range. Only in this way could sufficient data be obtained for a fuller survey of the problem so that theoretical workers could be better guided in their work. It is with this end in view that the present series of experiments has been carried out.

We shall deal with the results of the thermal conductivity measurements most conveniently by considering the specimens in their appropriate groups in the periodic classification of the elements. We shall consider each group in turn in which specimens were available and were measured. For those specimens whose electrical resistance was measured, either at liquid-hydrogen or at lower temperatures, the thermal conductivity was also calculated assuming the validity of the Wiedemann–Franz law at the appropriate temperature. This value is shown on the graphs by a ringed point. In most cases this falls very near to the experimental curve, showing that almost all the heat transport is due to electronic conduction and hardly any at all is due to lattice conduction.

Where the experimental curves show any sign of non-linearity they have been investigated to see whether they are of the form

$$1/K = W = \alpha T^2 + \beta/T,$$

as is suggested by the theory (equation (9)). This has been done by plotting WT against T^3 for the experimental points. Such curves are, in general, linear for the lower tem-

TABLE 1

specimen		source	purity (%)	ρ_{293}/ρ_{20}	remarks
aluminium	(Al1)	JM4899	99·994	279	annealed polycrystalline
antimony	(Sb1)	JM	—	6·37	annealed polycrystalline extruded wire
beryllium	(Be1)	A.E.R.E.	—	3·52	compressed powder, annealed
cadmium	(Cd1)	HS10547	99·9999	50·4	cast in glass, polycrystalline
	(Cd2)	HVPS8670	99·995	—	single crystal, hexagonal axis 79° to rod axis
cerium	(Ce1)	Prof. Spedding	99·6	1·93	polycrystalline
cobalt	(Co1)	JM	—	29·4	annealed polycrystalline
columbium	(Cb1)	JM4526	99·99	10·4	—
copper	(Cu1)	JM4234	99·999	85·3	annealed polycrystalline
gallium	(Ga42·1)	N.P.L.	—	92·1	single crystal, high-resistance direction
	(Ga42·2)	N.P.L.	—	111	single crystal, low-resistance direction
	(Ga42·3)	N.P.L.	—	106·5	single crystal, intermediate-resistance direction
gold	(Au1)	JM1916*a*	99·999	51·8	polycrystalline wire
indium	(In1)	JM4398	99·993	—	polycrystalline wire
iridium	(Ir1)	JM3441	99·995	225	annealed polycrystalline
iron	(Fe1)	JM4975	99·99 (excluding gases)	44·6 (run 1) 67·8 (run 2)	annealed polycrystalline
lanthanum	(La1)	Prof. Spedding	99·94	3·75	polycrystalline
lead	(Pb1)	Tadanac	99·998	—	single crystal
magnesium	(Mg2)	JM1703	99·95	140	annealed polycrystalline
manganese	(Mn1)	JM2472	99·99	1·47	annealed polycrystalline
molybdenum	(Mo1)	JM2331	99·95	36·2	—
nickel	(Ni1)	JM4884	99·997	80·9	annealed polycrystalline
palladium	(Pd1)	JM2134	99·995	34·1	annealed polycrystalline
platinum	(Pt1)	JM2157*b*	99·999	202	annealed polycrystalline wire
rhodium	(Rh1)	JM2357	99·995	63·1	polycrystalline wire
silver	(Ag1)	JM1722	99·99	30·9	polycrystalline wire
	(Ag2)	JM3351	purer than Ag1	142	annealed polycrystalline
tantalum	(Ta1)	JM3804	99·98	19·7	—
thallium	(Tl1)	JM2544	99·99	—	annealed polycrystalline wire
tin	(Sn1)	JM	99·997	—	single crystal
titanium	(Ti1)	A.E.I.	99·9	6·32	polycrystalline
	(Ti2)	A.E.I.	99·99	10·1	annealed polycrystalline
	(Ti3)	A.E.I.	99·99	—	single crystal
tungsten	(W1)	JM2260	99·99	38·0	annealed polycrystalline
uranium	(U1)	A.E.R.E.	—	10·6	—
vanadium	(V1)	JM	—	3·22	polycrystalline wire
zinc	(Zn2)	I.S.C.	99·997	—	single crystal, hexagonal axis at 80° to rod axis
	(Zn3)	I.S.C.	99·997	—	single crystal, hexagonal axis at 13° to rod axis
	(Zn4)	I.S.C.	99·997	—	single crystal, hexagonal axis at 13° to rod axis
Zirconium	(Zr1)	JM3062	~98	21·2	annealed polycrystalline
	(Zr2)	Metro Vickers	~98	42·5	annealed polycrystalline

JM = Johnson, Matthey. H = Hilger.
A.E.I. = Associated Electrical Industries Research Laboratories, Aldermaston.
I.S.C. = Imperial Smelting Corporation, Avonmouth.
Tadanac lead from Messrs Goodlass Wall and Lead Industries Ltd.

peratures, showing that in this region the relation (9) is applicable. The constant α, which is the slope of the WT curve, has been calculated. While in the cases where (9) holds accurately it has been possible to do this to about 2 %, in general the error in α might be as much as 5 %. The value of β, which is the intercept of the curve on the WT axis, has also been determined. This is a measure of the impurity scattering that is present in the particular specimen measured, whereas α should be a constant for a given metal.

TABLE 2

specimen	length (cm)	diam. (cm)	$10^5\alpha$	β
Ag1	2·85	0·122	4·3	1·6
Ag2	2·8	0·133	5	0·3
Al1	2·97	0·394	3·2	0·23
Au1	$F = 497$		19	1·13
Be1	2·01	0·231*	—	177
Cb1	3·03	0·470	50	58
Cd1	$F = 160$		145	0·3
Cd2	3·02	0·0272*	122†	0·02
Ce1	1·085	0·38 square	—	900
Co1	3·03	0·204	10·5	7·9
Cu1	2·99	0·302	2·5	0·35
Fe1	2·89	0·202	10·2 (run 1)	9·6 (run 1)
			9·5 (run 2)	5·9 (run 2)
Ga42·1	2·92	0·223	160 (up to 7°K)	4·7
Ga42·2	2·45	0·218	23 (up to 7°K)	0·165
Ga42·3	$F = 94·4$		87 (up to 7°K)	2·22
In1	3·08	0·158	185	0·35
Ir1	2·51	0·205	4·6	0·75
La1	$F = 4·65$		—	740
Mg2	2·7	0·161	8·5	1·05
Mn1	$F = 17·76$		—	1200
Mo1	2·85	0·52	7·5	6·7
Ni1	2·92	0·305	10·4	4·6
Pb1	3·02	0·0264*	290 (up to 5°K)	0·1
Pd1	2·82	0·152	41	11·7
Pt1	2·97	0·104	43	0·35
Rh1	1·04	0·051	10·7	1·38
Sb1	1·625	0·163	—	—
Sn1	2·95	0·389	60 (up to 5° K)	0·12
Ta1	3·0	0·225	79	25
Ti1	3·07	0·246	—	290
Ti2	1·56	0·242	—	170
Ti3	1·6	0·0306*	454	81·6
Tl1	2·99	0·16	537	0·1
U1	2·95	0·203	790	93
V1	0·725	0·0995	124	310
W1	2·96	0·401	9·3	5·8
Zn2	2·86	0·0215*	34	0·7
Zn3	1·95	0·0230*	31	0·6
Zn4	2·75	0·0234*	30	0·6
Zr1	2·83	0·326	127	76
Zr2	3·07	0·44	125	33·8

* Cross-sectional area in cm^2. F = form factor.
† See footnote on p. 494.

A list of the specimens, together with their sources, purity and remarks regarding their heat treatment and crystalline state, is given in table 1. The dimensions of the specimens, together with the values of α and β, are given in table 2. Samples designated by JM were made from Johnson, Matthey spectrographically standardized metals.

Some of these results have already been briefly reported (Mendelssohn & Rosenberg 1952*a*, *b*). These, however, were only provisional values, and in some cases they have been slightly modified after more accurate computation.

8·2. *The metals of group* 1*b*

In this group one specimen each of copper and gold and two specimens of silver were measured. The conductivity curves are drawn in figure 4. They all show the characteristic curve to be expected from a pure metal. At low temperatures there is a linear section which passes through the origin. It then rises to a maximum in the temperature range covered, and beyond this it falls first steeply and then more gradually.

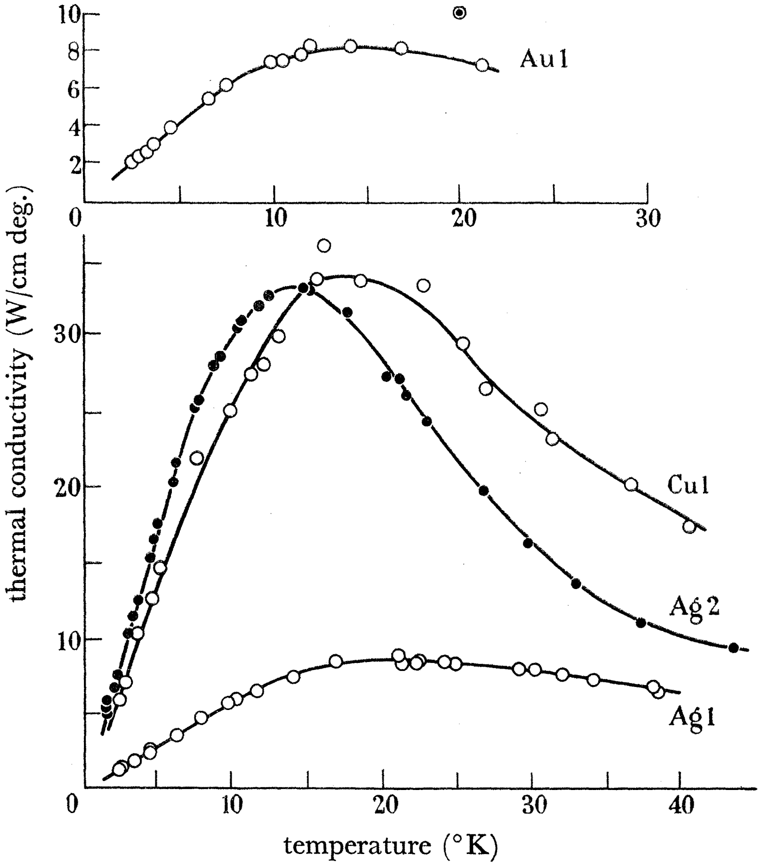

Figure 4. The thermal conductivity of the specimens of copper, silver and gold. The ringed point for Au 1 shows the thermal conductivity as calculated from the electrical resistance assuming the validity of the Wiedemann–Franz law.

Copper

This specimen, Cu 1, was made from sample JM 4234 which was turned down to a diameter of 2·99 mm and then annealed *in vacuo* for several hours at 800° C. Unfortunately, it was still too thick to measure the high conductivity very accurately, and this accounts for the scatter in the points. Berman & MacDonald (1952) have obtained a thinner specimen from the same batch of copper and their curve has a much higher and sharper maximum at the same temperature. The two curves agree at the higher temperatures. The higher maximum which Berman & MacDonald have obtained is presumably due to the difference in annealing and preparation of their specimen. The measurements give a value for α of $2{\cdot}5\times10^{-5}$, and this agrees with that of Berman & MacDonald.

Silver

Two silver specimens were investigated. The first, Ag 1, was an unannealed polycrystalline wire JM 1722 which had a purity of 99·99 %. The second, Ag 2, was made from JM 3351. Although no figures were available for Ag 2 it was stated to be considerably purer than Ag 1. Ag 2 was made from a rod with a diameter of about 5 mm by rolling it to a sheet about 1 mm thick. This was cut into thin strips, and one of these was drawn down to a wire 1 mm in diameter. This wire was annealed *in vacuo* at 750° C for several hours. Comparison of the curves for Ag 1 and Ag 2 shows how for Ag 2, the purer specimen, the conductivity maximum is shifted to a lower temperature and is very much higher. It is nearly as great as that of Cu 1. The two silver curves tend to the same value of conductivity at higher temperatures.

Up to about 17° K α is $4{\cdot}3\times10^{-5}$ for Ag 1 and 5×10^{-5} for Ag 2. For the range up to 35° K better values are 7·3 and $6{\cdot}2\times10^{-5}$ respectively. We shall on other occasions have to note more than one value of α, and while the theory would suggest that it is that for the lowest temperature range which is of the greatest interest, nevertheless—since the higher portion of the $WT\sim T^3$ curve is also linear—it would seem that the slope of this section might also be significant from a theoretical point of view. The values for α agree approximately with those of White (1953 *a*), although he finds a much greater variation in α between annealed and unannealed specimens.

Gold

Au 1 was an unannealed polycrystalline wire JM 1916 *a* which had a purity of 99·999 %. The conductivity curve with a broad maximum is shown in the upper section of figure 4. The thermal conductivity as calculated from the electrical resistance at the temperature of liquid hydrogen is shown by a ringed point above the curve. The position of this point shows that the region of constant residual electrical resistance had not been reached, because if it had, the point would have fallen on to the continuation upward of the linear part of the conductivity curve. While in this particular case, therefore, this reading is of no great interest, it is mentioned here by way of introduction to those cases where the measurement of the electrical resistance is of use in determining the electronic thermal conductivity. Electrical resistance points, similar to that for Au 1, were obtained for Cu 1 and Ag 2, but these were too high to be shown on the graph. From the WT plot, α in gold has the value 19×10^{-5}. This is similar to that obtained by White (1953 *b*).

8·3. *The metals of group* 2*a*

Two metals were available, beryllium and magnesium. Their conductivity curves are shown in figures 5 and 6.

Beryllium

The only pure beryllium that was obtainable was from the Atomic Energy Research Establishment, and was in the form of a ring made from compressed powder. This ring was cut in two and one of the semicircles so formed was used as the specimen. Holes of size 12 B.A. were tapped at either end of the specimen and brass screws were tightly fixed into these to act as thermometer contacts. A small copper clamp connected the cold end of the specimen to the point of attachment in the apparatus. The specimen, Be1, was annealed *in vacuo* for several hours at 1100° C.

Beryllium has a very high Debye temperature (1160° K), and therefore one would not expect to discover a maximum in the conductivity in the range of temperatures covered here and this is confirmed in the graph (figure 5). Because the specimen was made from a powder, the conductivity is rather low, being of the order of 10^{-1}W units. This is because the impurity scattering term is very high. Nevertheless, it can be seen that the electrical resistance measurement gives a point which is nearly on the experimental curve, showing that in spite of the low conductivity it is still due almost entirely to electronic heat transport. Since the graph is approximately linear over most of the range it has not been possible to calculate a value of α. The beryllium single crystals used by Grüneisen and his co-workers (Grüneisen & Adenstedt 1938; Grüneisen & Erfling 1940) had a conductivity of 30 W units at 20° K, and it is very disappointing that such crystals are not available at the moment because then much more information could have been obtained. Grüneisen & Adenstedt (1938) have shown by measurements in a magnetic field that their specimens had a lattice conductivity of about 0·1 W unit, and Powell (1953) in measurements at room temperature and above shows that his specimens also have an appreciable lattice conductivity. From the present electrical measurements, however, it seems unlikely that the lattice contribution to the thermal conductivity at 20° K is greater than 0·01 W unit.

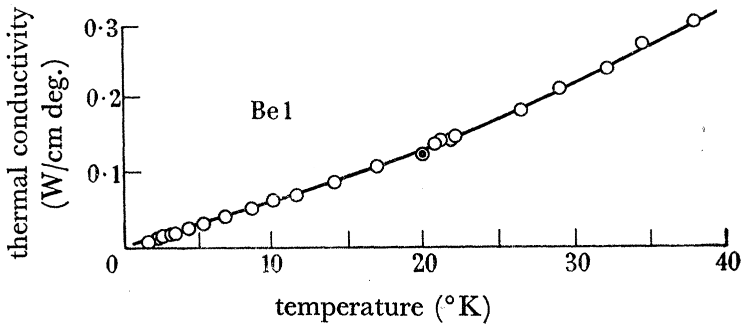

FIGURE 5. The thermal conductivity of the beryllium specimen. The ringed point shows the thermal conductivity as calculated from the electrical resistance assuming the validity of the Wiedemann–Franz law.

Magnesium

Mg2 was a polycrystalline rod of JM1703 which had been annealed *in vacuo* at 500° C for 6 h. Like beryllium it would not take solder and thermal contact was made to the thermometers by two small copper clamps fixed on to the specimen a few centimetres apart. Since it was known that some specimens of magnesium, including this batch of metal, exhibited a minimum in the electrical resistivity at low temperatures (MacDonald & Mendelssohn 1950), it was of interest in this case to see whether there was any corresponding effect in the thermal conductivity. For this reason the electrical resistance of this specimen was measured at the same time as its thermal resistance in the manner described in § 6. The thermal and electrical curves are shown in figure 6, and as has already been reported (Rosenberg 1954*a*) a minimum was indeed confirmed in the electrical resistance, at about 6° K. In the same region the thermal conductivity rises above the straight line through the origin which is shown dashed in the graph. The effect is shown up much more clearly, however, when WT is plotted against T^3. This, as has been explained, should give a straight line up to about $\theta/10$. Figure 7 shows that while that is so over most of the range, at the lower temperatures the value of WT drops below this line, passes through a minimum at about 6° K and then rejoins the line again. If we plot ΔW, i.e. the amount by which W varies from the theoretical straight line, against temperature, the graph drawn in figure 8 is obtained, and this clearly shows a minimum at 6° K of about 4 % of W.

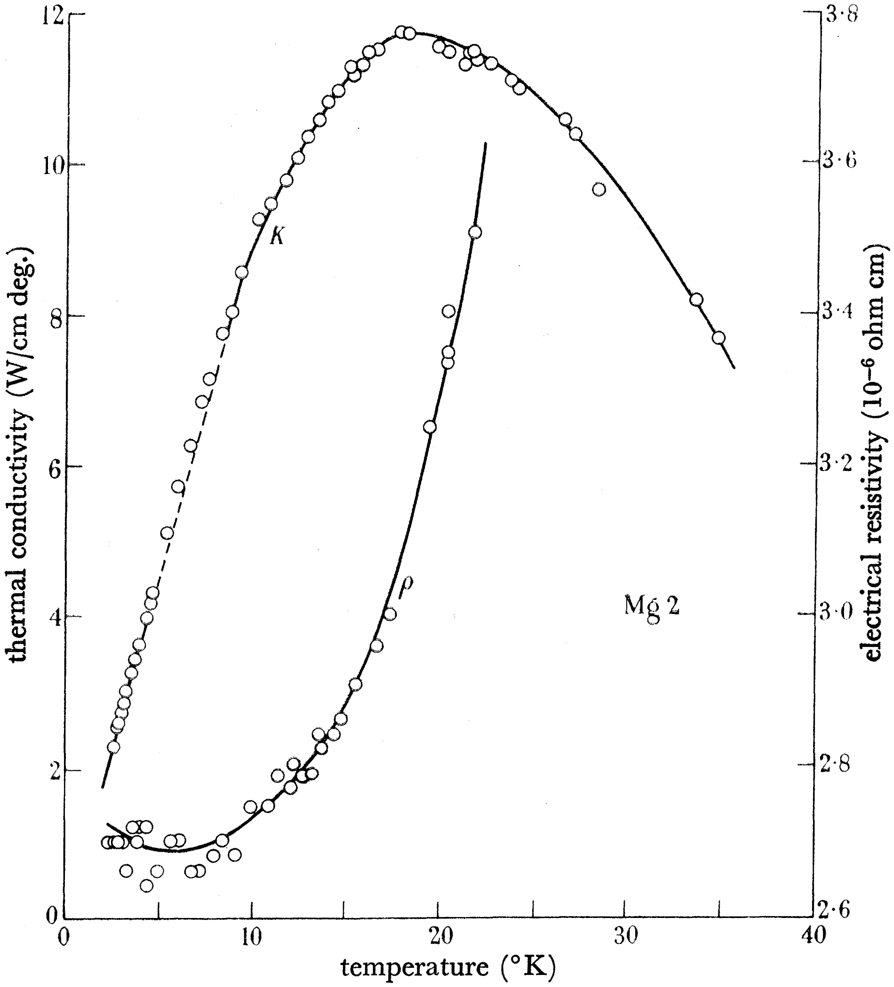

FIGURE 6. The thermal conductivity, K, and the electrical resistivity, ρ, of the magnesium specimen. This shows the minimum in the electrical resistance and the corresponding departure from linearity in the thermal conductivity.

In the electrical resistance, ρ, the minimum is about 3 % below the residual resistance as deduced from the measured points above 10° K by plotting ρ against T^5. Thus it is clear that corresponding effects are shown in both the residual electrical resistivity and in the thermal conductivity.

The mechanism which produces the minimum has not, as yet, been explained, although there seems to be no doubt that it is due to very small amounts of certain impurities (Mendelssohn 1951; MacDonald 1952). In the specimen used it seems likely that the minimum is due to a manganese impurity of about 0·03 %.

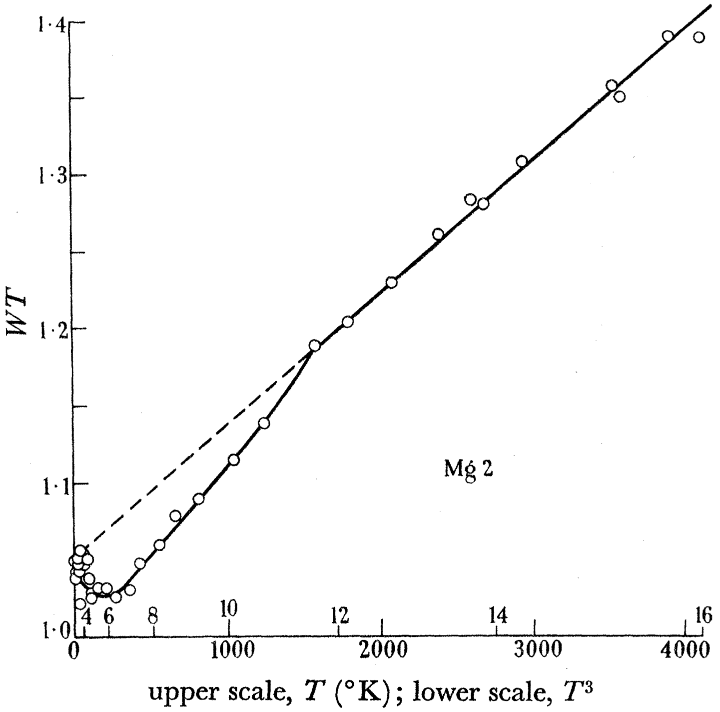

FIGURE 7. The graph of WT against T^3 for Mg 2 showing the minimum in the curve.

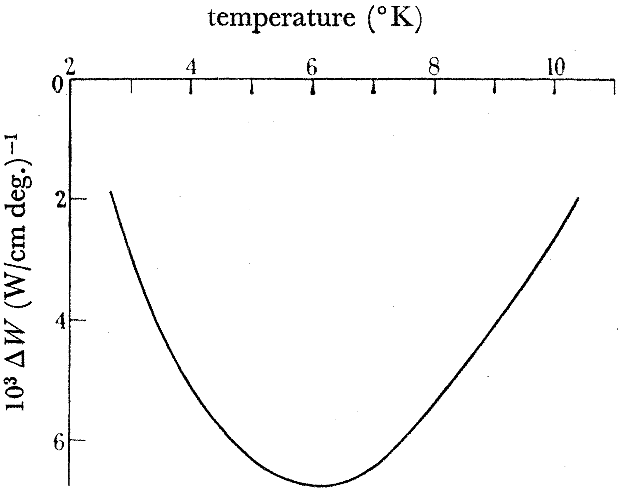

FIGURE 8. The graph of ΔW against T for Mg 2.

Since comparable effects were found in both the electrical and thermal conductivities no anomaly was found in the Lorenz number, L, which is shown in figure 9. In the temperature range covered, L rises with decreasing temperature, flattening off to a constant value at about 5° K. Below this temperature the Wiedemann–Franz law is valid.

It will be noted that this constant value of L is $2{\cdot}6\times10^{-8}$, being slightly higher than the theoretical value of $2{\cdot}45\times10^{-8}$.

Experiments by Kemp, Sreedhar & White (1953) on magnesium failed to reveal any anomaly in the impurity resistance.

The value α as deduced from the linear part of the WT curve is $8{\cdot}5\times10^{-5}$.

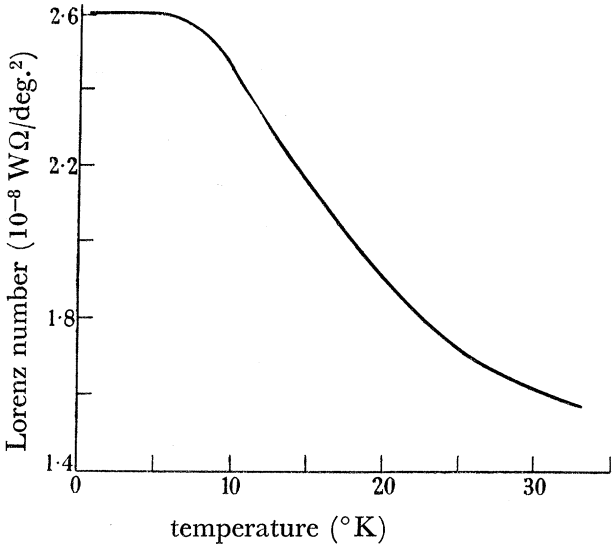

FIGURE 9. The value of the Lorenz number, L, for the magnesium specimen.

8·4. *The metals of group 2b*

Three single-crystal specimens of zinc and one single-crystal and one polycrystalline specimen of cadmium were investigated. Their conductivity curves are shown in figures 10 and 11. It will be noted that all specimens show a sharp maximum below 10°K.

Zinc

All three single crystals were prepared from the same batch of 99·997 % purity metal supplied by the Imperial Smelting Corporation, Avonmouth. They were made by Dr A. J. Goss of the University of Southampton. As originally prepared they were too thick for accurate measurements, and they were made thinner by partly dissolving them in hydrochloric acid. The cadmium single crystal was treated in the same way. Zn 2 had its hexagonal axis at 80° to the rod axis, whereas both Zn 3 and Zn 4 had their hexagonal axes at 13° to the rod axes. This was the nearest approach that could be made easily to a set of specimens with their crystal axes parallel to and perpendicular to the rod axes.

The conductivity curves in figure 10 show that the low-temperature linear section of the graph is the same for each specimen, indicating that the impurity scattering term is the same for each, as indeed it should be. At higher temperatures, however, Zn 3 and Zn 4 both have a higher conductivity than Zn 2, this being about 10 % greater at the maximum. Beyond this, the curve for Zn 3 and Zn 4 falls more steeply than that for Zn 2 which it crosses at about 27°K. Above this temperature Zn 2 has the greater conductivity. It will be noted that the curves for Zn 3 and Zn 4 do coincide fairly well over the whole experimental range.

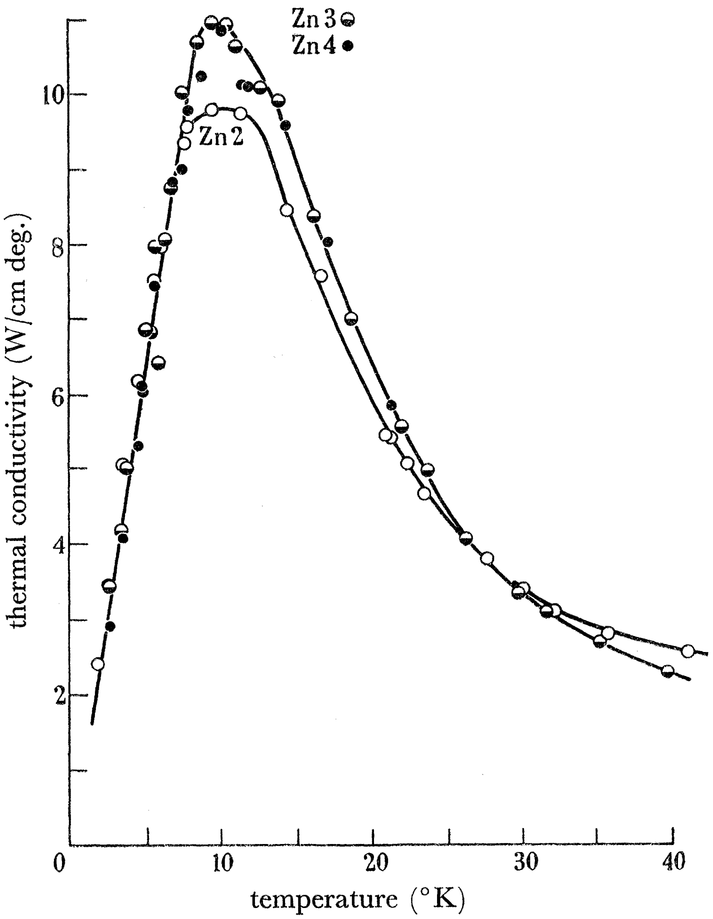

FIGURE 10. The thermal conductivity of the zinc specimens.

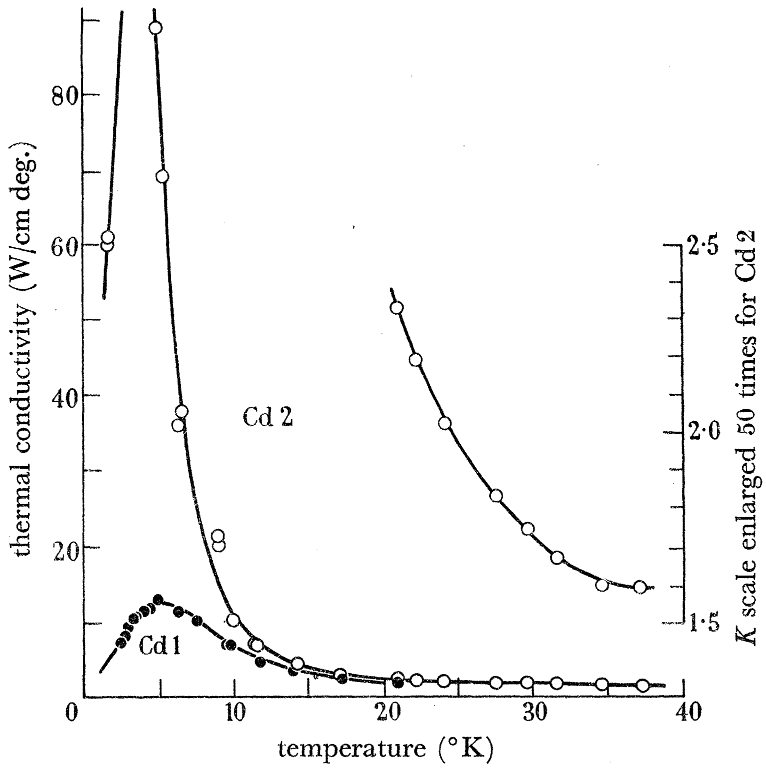

FIGURE 11. The thermal conductivity of polycrystalline cadmium, Cd 1, and the single crystal of cadmium, Cd 2. The inset shows the high-temperature curve for Cd 2 with the conductivity scale enlarged 50 times.

Anisotropy in the electrical and the thermal conductivity of both zinc and cadmium has been observed down to liquid-hydrogen temperatures by Grüneisen & Goens (1932), but since the maximum in the thermal conductivity was not reached in this work, their measurements did not show so marked an effect as does the present work. It will be noted that at high temperatures the thermal conductivity is smaller in the direction parallel to the hexagonal axis. While the general problem of anisotropy in metals has been treated (see Boas & Mackenzie 1950), the magnitude of the anisotropy of the thermal conductivity and its dependence on lattice constants has, so far, not been calculated.

Graphs of WT give values for α of 34×10^{-5} for Zn 2, 31×10^{-5} for Zn 3 and 30×10^{-5} for Zn 4.

Cadmium

The polycrystalline specimen, Cd 1, was cast from Hilger HS 10547, which was stated to have a purity of 99·9999 %. Cd 2 was a single crystal whose hexagonal axis was at 79° to the rod axis. It was made from Hilger VPS 8670, which had a purity of 99·995 %. The conductivity curves in figure 11 show how large an influence is the effect of having a single-crystal specimen, since Cd 1, the polycrystalline sample, was much purer than Cd 2. Nevertheless, whereas the maximum conductivity of Cd 1 was about 12 W units, that for Cd 2 was between 150 and 200 W units. This high conductivity is very much dependent on having a strain-free specimen, as was shown during later experiments when the specimen, Cd 2, had been removed from the apparatus and was bent slightly on being replaced. The maximum conductivity was then found to have been reduced to about 70 W units, which, although still high, is considerably less than that found in the first experiments.

It will be noted that in spite of the large difference in their conductivities at the lower temperatures, both specimens have approximately the same conductivity at higher temperatures. This is in accord with the theoretical requirement that at high temperatures the conductivity is dictated by lattice scattering which will, of course, be the same for all specimens. To avoid any misunderstanding, it should be emphasized that the difference in the conductivities at low temperatures is due to Cd 2 having a smaller impurity scattering term. It has no connexion with the lattice scattering term, although the lower 'impurity' in this case is due to the single-crystal nature of the specimen.

Up to 14° K the WT curves for both specimens are linear, giving $\alpha = 145\times10^{-5}$ for Cd 1 and 122×10^{-5} for Cd 2*. The difference in the two values might be due either to an anisotropy, which will almost certainly occur in cadmium similar to that which was found in zinc, or to an error in the form factor for Cd 1 which was difficult to measure.

8·5. *The metals of group* 3

In this group aluminium, gallium, indium and thallium have been investigated. The conductivity curves are given in figures 12 and 13. Lanthanum, also in group 3, has been measured, but this will be dealt with at a more convenient point later (see § 8·13).

---

* See footnote on p. 494.

Aluminium

The specimen Al 1 was a polycrystalline rod of JM 4899 which had been annealed *in vacuo* at 600° C for several hours. Its purity was 99·994 %. The conductivity curve in figure 12 shows a maximum of over 40 W units at about 17° K. Plots of WT against T^3 do not give a strictly linear curve over the whole range. The slope appears to decrease as T^3 increases. The most representative value for α, covering the points up to 35° K is $3{\cdot}2\times10^{-5}$. This seems to be the best one to take, since with a Debye temperature of 400° K the value of α should be the one which does cover the full range to which the simple theory is supposed to apply, i.e. up to about $\theta/10$. This value of α does not agree exactly with that given by Andrews, Webber & Spohr (1951) who investigated three specimens of aluminium, one of which was from Johnson, Matthey. This specimen gave a conductivity curve very similar to our Al 1, but the value of α is given as $2{\cdot}7\times10^{-5}$, which is slightly lower than our value. A rough estimate of the lattice scattering term, W_0, has been made for Al 1, and it does seem to vary as $T^{2\cdot2}$ over a large part of the temperature range, rather than as T^2. This would account for the non-linearity of the WT curve. Such an increase in the power of T has also been suggested by White (1953 *a*) in some experiments on silver.

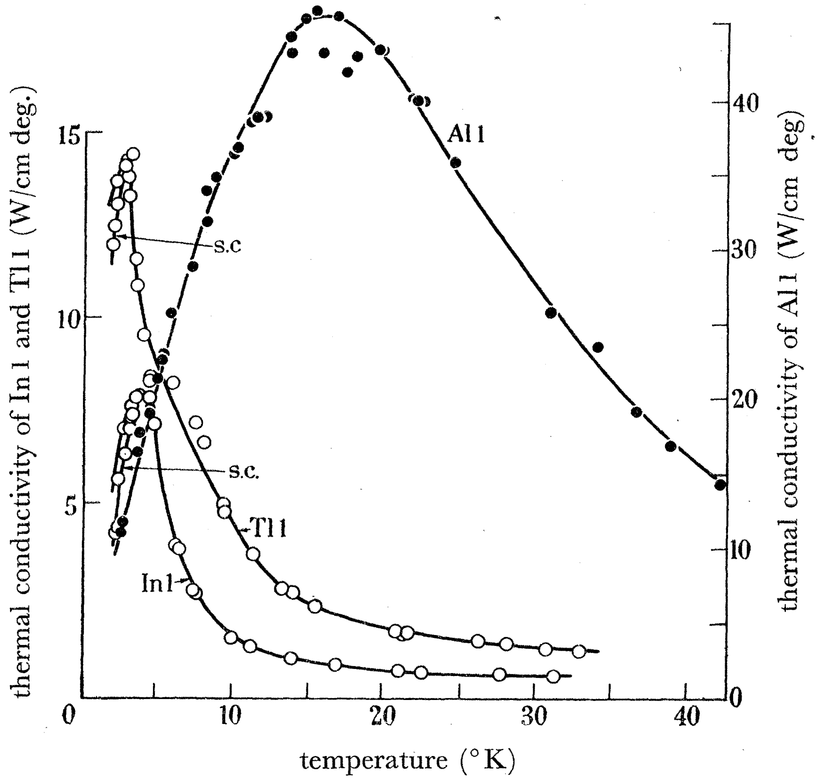

FIGURE 12. The thermal conductivity of the aluminium, indium and thallium specimens. Measurements for thallium and indium are shown for both the normal and superconducting (s.c.) states.

Gallium

Gallium exhibits considerable anisotropy in its electrical and thermal resistances at room temperature (Powell 1951) and the electrical anistropy has been found to persist to low temperatures (Olsen-Bär & Powell 1951). It was therefore of interest to see whether the thermal resistance was also anisotropic at low temperatures. Three single crystals were prepared by Dr R. W. Powell of the National Physical Laboratory. These had their axes parallel to the directions of high, low and intermediate electrical resistivity and are designated Ga 42·1, Ga 42·2 and Ga 42·3 respectively. They were all made from the same batch of metal. The thermal conductivity curves are shown in figure 13. As has been briefly reported earlier (Rosenberg 1954*b*), there is a strong anisotropy in the conductivity of the metal, the highest conductivity being in that specimen which has the lowest electrical resistance. There is a similar correspondence for the thermal conductivity in the intermediate and high electrical resistance directions.

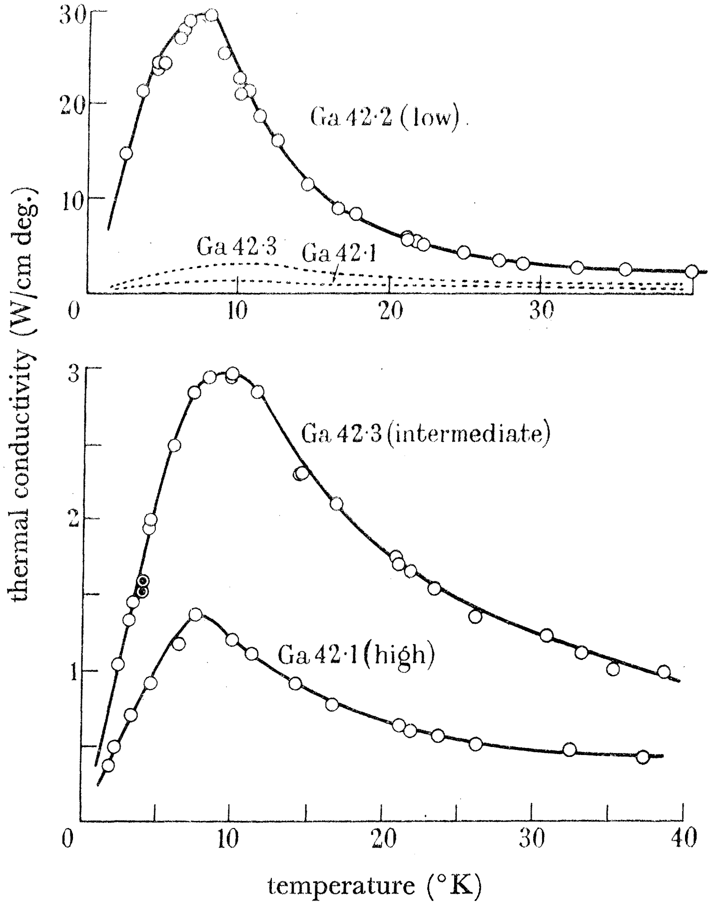

FIGURE 13. The thermal conductivity of the gallium single crystals which were grown along the directions of high, low and intermediate electrical resistance.

The ratio of the electrical resistivities in the three directions is given as 1:2·1:6·5 at room temperature and 1:2·1:8 in the range 4 to 20°K (Olsen-Bär & Powell 1951). The electrical resistance ratio of our specimens at 20°K was 1:2·7:8·9. The thermal resistances of our specimens at the highest temperatures measured, about 40°K, have a ratio of approximately 1:2·3:5·2. At lower temperatures the thermal resistances of the two higher resistance specimens Ga 42·1 and 42·3 are in almost the same ratio as they were at 40°K, but the low-resistance specimen, Ga 42·2, decreases its resistance to a much greater extent. This can be seen from the fact that at the maximum conductivities of the specimens, the resistances are in the ratio 1:10:23. Thus, while in broad outline the thermal resistance does follow the anisotropy of the electrical resistance, particularly for the two higher resistance specimens, in detail this does not seem to be an accurate guide. It is of course possible that the two higher resistance specimens had been strained and that this had reduced their conductivities in the low-temperature region. Then, ideally, their conductivities should have been higher and more in accord with the very high conductivity of Ga 42·2. This seems unlikely, however, since they would both have to be strained just to the extent that their resistances remained in the same ratio as the temperature was decreased. Nevertheless, inspection of table 2 shows that the change in the ratio is actually due to the impurity scattering terms, β, and not to α, so the possibility of strained specimens must be considered.

The values of α have been calculated for the three specimens from the WT curves. None of the curves are strictly linear; they all initially bend away from the T^3 axis. Two slopes are therefore given. One covers the range up to 7° K and the other from 7 to 17° K. These values are (in the order 42·2, 42·3, 42·1), 23, 87, 160×10^{-5} up to 7° K and 35, 142, 367×10^{-5} from 7 to 17° K. It was of interest to see how the ratios of these values of α compared with the previous ratios mentioned. They are 1:3·8:7·0 below 7° K and 1:4·0:10·5 from 7 to 17° K. Once again there is broad general agreement but this is only qualitative.

Electrical resistance measurements at 4·2 K were taken on Ga 42·3, and the thermal conductivity points calculated from these show good agreement with the experimental curve.

The difficulty of comparing the thermal conductivities of three soft single crystals which must each be fitted into the apparatus with as little damage as possible will be appreciated. It should be noted, however, that any inadvertent damage would only affect the impurity scattering term, and that the lattice scattering term, α, should remain unchanged by this treatment. Nevertheless, it is evident both from these experiments and from those of Olsen-Bär & Powell that there is an anisotropic effect not only in the lattice scattering resistance, W_0, but also in the impurity resistance, W_i. This seems to indicate that the distribution of the impurities, either chemical or physical, is not homogeneous but is concentrated along certain preferred directions in the crystal.

Indium

In 1 was an unannealed polycrystalline wire of JM 4398. The thermal conductivity is shown as the lowest curve of figure 12. It rises to a sharp maximum of 8 W units at about 5° K. Below the superconducting transition temperature in zero field, 3·37° K, measurements were taken in both the normal and superconducting states, a magnetic field being used to destroy the superconductivity. This specimen had an appreciable magnetoresistance (see Mendelssohn & Rosenberg 1953), and the conductivity in the normal state had to be corrected for this. Measurements were taken in higher magnetic fields so that the value of the conductivity in the normal state could be extrapolated to that in zero magnetic field.

The value of α for this metal in the range up to 12° K is 185×10^{-5}. This compares well with that given by Hulm (1950) of 189×10^{-5}. Hulm's specimen was not so pure as ours, as it had 0·1 % impurity and did not exhibit a maximum in the conductivity.

Thallium

This specimen, Tl 1, was polycrystalline and was made from JM 2544 which had been annealed *in vacuo* for several hours. It was coated with celluloid varnish to prevent oxidation. The thermal conductivity curve is shown in figure 12, and it will be seen that it closely resembles that of In 1, except that its maximum is much sharper and occurs at a slightly lower temperature. This metal becomes superconducting at 2·38° K, and since this is at the lower end of our range of measurements, only one point for the normal state is shown. The general shape for this curve and the one for In 1 is characteristic of a pure metal which has a low Debye temperature (90° K for Tl and 100° K for In). As the temperature is decreased, the thermal conductivity only increases appreciably below 20° K and then it rises to a sharp maximum. This behaviour is contrasted by that of the aluminium curve on the same figure. The Debye temperature for aluminium is about 400° K and the difference in the curves is readily apparent. The conductivity of Al 1 is already rising steeply at 40° K and, although the specimen is very pure, as is shown by its high conductivity, it has a broad maximum at a much higher temperature than those of the other two metals.

The WT curve for Tl 1 has a pronounced bend towards the T^3 axis above about 10° K, which again one would expect from a specimen with a low Debye temperature (see § 9). Up to 7° K the curve is quite linear and the value of α is 537×10^{-5}.

8·6. *The metals of group* 4*a*

In this group three specimens of titanium and two of zirconium have been investigated. Their conductivity curves in figures 14 and 16 show that they all have a much lower conductivity over the range measured than have any of the other specimens (except the compressed powder, Be 1) which have so far been discussed.

Titanium

All these specimens were obtained from the Associated Electrical Industries Research Laboratories and were very pure samples prepared by the Van Arkel process. Ti 1 was an unannealed polycrystalline rod which had a purity given as 99·9 %. Ti 2 was a polycrystalline rod with a purity given as 99·99 %, and it was annealed *in vacuo* for 20 h. For this process it was enclosed in a tube of commercial titanium to avoid the risk of contamination from the quartz outer container. It is understood that the most troublesome impurities are gaseous ones; oxygen, in particular, affects the physical properties of the metal. Ti 3 was a single crystal prepared by the method described by Churchman (1953). It had a Vickers pyramid hardness of 94, from which it is deduced that the oxygen and nitrogen impurity was about 0·01 %.

The thermal conductivity curves for Ti 1 and Ti 2 (figure 14) show that both of them have a very low conductivity, although that of the annealed and perhaps purer specimen, Ti 2, is nearly twice that of Ti 1. Both graphs are linear, passing through the origin. There is no sign of curvature at all, which indicates that the conductivity is limited by impurity scattering over the entire range observed. Because of this it was not possible to calculate a value of α for these specimens.

The electrical resistance measurements which were taken are rather interesting. The thermal conductivity at 20° K as calculated from these is shown in the figure, and it can be seen that in both cases it is about 0·01 W unit below the experimental value of the conductivity at this temperature. At first sight it might appear that this might be due to there being an appreciable amount of lattice conductivity present in the metal, particularly as its total conductivity is so low. The amount of this lattice conductivity would be the difference between the experimental curve and that derived from electrical measurements, since the latter would, of course, only give the electronic contribution. The fact that this difference is almost the same for both specimens suggests that each specimen has the same conductivity which is less dependent on impurities than is the electronic conductivity. This explanation, however, does not seem possible. Assuming that we have reached the region of constant residual electrical resistance and that the Wiedemann–Franz law holds, the electronic thermal conductivity is linear with the temperature and should in fact be a straight line passing through our ringed point and the origin. The difference between this line and our experimental curve would then give the lattice conductivity. Since the experimental curve is linear this would mean that the curve of the lattice conductivity would also be linear. No mechanism has, as yet, been suggested for this to occur. In a metal the lattice conductivity is usually proportional to T^2, being limited by the scattering of lattice waves by the electrons. Impurity scattering of the lattice waves gives a term in T^{-1} (see Berman 1953). There does not seem to be any possibility of a linear lattice conductivity.

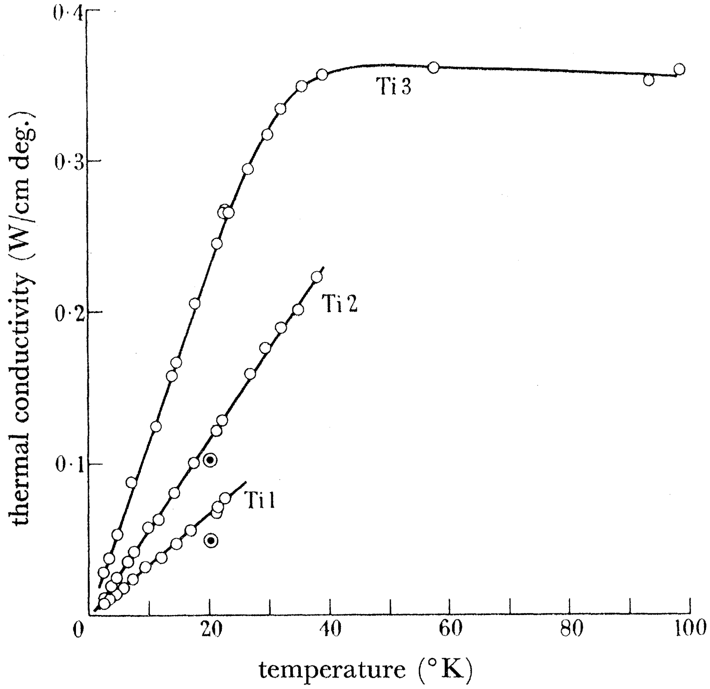

FIGURE 14. The thermal conductivity of the titanium specimens. Ti 1 and Ti 2 were polycrystalline and Ti 3 was a single crystal. The ringed points show the thermal conductivity for Ti 1 and Ti 2 as calculated from the electrical resistance, assuming the validity of the Wiedemann–Franz law.

When the opportunity of measuring a single crystal of titanium arose it was undertaken with great interest, in the main to see whether it, too, would show a very low thermal conductivity, and also to see what kind of results the electrical measurements would give. The thermal and the electrical conductivities were measured up to 90° K, and the results are shown in figures 14 and 15 respectively. It will at once be seen that while the thermal conductivity is larger than before, it is still very low, being only about twice that of Ti 2. At about 40° K it flattens off to an approximately constant value. It seems therefore that the small amount of gaseous impurity is still limiting the conductivity, unless the low value is a fundamental property of the metal itself, which seems unlikely. From the results on Ti 3 we can calculate a value for α of 454×10^{-5}. The electrical resistance of the specimen indicates that the region of the residual electrical resistance is reached just below 20° K.

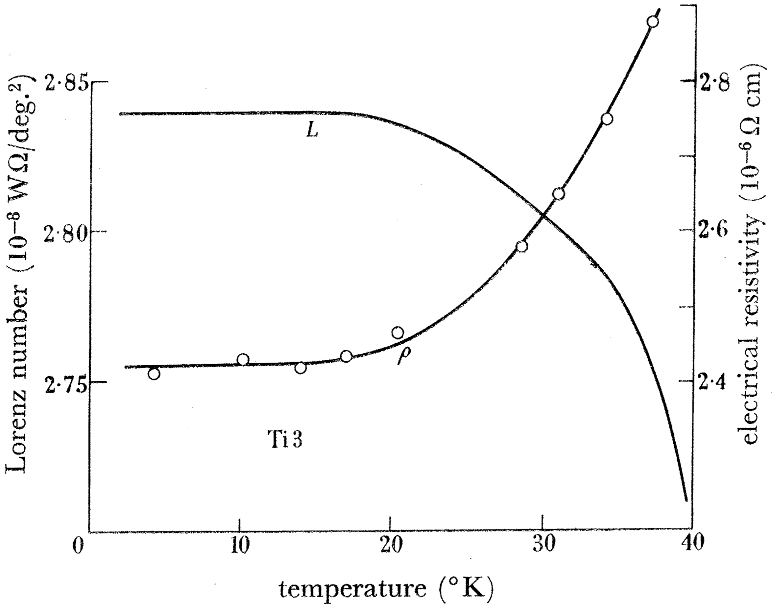

FIGURE 15. The value of the Lorenz number, L, and the electrical resistivity, ρ, for the titanium single crystal, Ti 3.

The Lorenz number has been calculated and this is also shown in figure 15. It can be seen that this reaches a constant value of $2{\cdot}84 \times 10^{-8}$ at 18° K. This is almost the same as the value of L calculated from the electrical measurements on Ti 1 and Ti 2. These come out as 2·81 and $2{\cdot}84 \times 10^{-8}$ respectively. This correspondence confirms the fact that there can be no appreciable lattice contribution present in any of the specimens, since it is highly unlikely that the lattice contribution should increase in the same proportion as the electronic conductivity so as to give the same value of L in each case. It thus seems that while the Wiedemann–Franz law holds in the low-temperature region, the Lorenz number is higher than that predicted by theory. A similar effect will be described for zirconium, vanadium, manganese and cerium, which also have low thermal conductivities.

Zirconium

Zr 1 was a rod of JM 3062 which had been annealed *in vacuo* at 1150° C for several hours. Zr 2 was a piece of the metal from Metropolitan Vickers, prepared by the Van Arkel process. Neither of these specimens was as pure as the other metals which we have described, as they contained hafnium impurity to the extent of about 2 %. This might account for the low conductivities of the specimens as is shown in figure 16. On the other hand, the very great similarity in structure and properties of hafnium and zirconium, as is evident by the great difficulty presented in their separation, might not cause the conductivity to be reduced as much as one would otherwise suppose; i.e. the hafnium might not have as great a scattering effect as any other impurity atom.

Zr 2 was composed of quite large crystallites visible to the naked eye. Apart from the hafnium present it was understood to be very pure, although exact figures were not given. Both the electrical and thermal conductivities were measured for this specimen and they are shown in figure 16. Figure 17 shows the value of the Lorenz number, L. It will be noted that the thermal conductivity is about twice that of Zr 1, and that a broad maximum occurs in the experimental range. The value of L increases as the temperature is lowered, and it is interesting to find that it reaches a constant value of $2{\cdot}75\times10^{-8}$. As with the case of titanium this is again higher than the theoretical value. It will be recalled that the limiting value of L to Ti 3 was $2{\cdot}84\times10^{-8}$.

The values of α from plots of WT are 127×10^{-5} for Zr 1 and 125×10^{-5} for Zr 2.

8·7. *The metals of group 4b*

Tin and lead were the metals of this group which were investigated. Their conductivity curves are shown in figures 18 and 20. Both metals are superconductors, and their behaviour below the superconducting transition temperatures, T_c, was determined in both the superconducting and the normal states. The specimens used were single crystals prepared by Dr A. J. Goss of the University of Southampton.

Tin

This specimen was made from Johnson, Matthey metal with a purity given as 99·997 %. The thermal conductivity curve in figure 18 shows quite a high maximum of 25 W units at about 5° K. Below 3·69° K, the transition temperature, the superconducting curve drops sharply away from the normal curve, although there is no evidence of a discontinuous change of slope at the transition temperature. The normal curve was measured in the usual way by applying a field sufficient to destroy the superconductivity. This was then removed and the conductivity was again measured in zero field. These last points are shown on the graph by a half-filled circle, and it is seen that they all fall exactly on the superconducting curves showing that no magnetic field was frozen into the specimen. This is quite a sensitive test for the presence of any frozen-in flux.

The curve of WT against T^3 (figure 19) is linear up to about 5° K, and then the slope tends to increase before the curve bends over towards the T^3 axis at about 15° K. The value of α up to 5° K is 60×10^{-5}. Between 5 and 14° K it is 116×10^{-5}. Hulm (1950) gives α as $39{\cdot}2\times10^{-5}$ for a polycrystalline specimen with a purity of 99·996 %. This is his specimen Sn 2. On the other hand, the value of α which he gives for his Sn 3 (purity 99·967 %) is 57×10^{-5}. This is much more in accord with our value up to 5° K of 60×10^{-5}. It is possible that our specimen has not its stated purity because although it is a single crystal and was supposed to be slightly purer than Hulm's Sn 2, nevertheless, his specimen has double the conductivity of ours. Even if this were so, it would not explain a discrepancy in the value of α, which should be independent of purity.

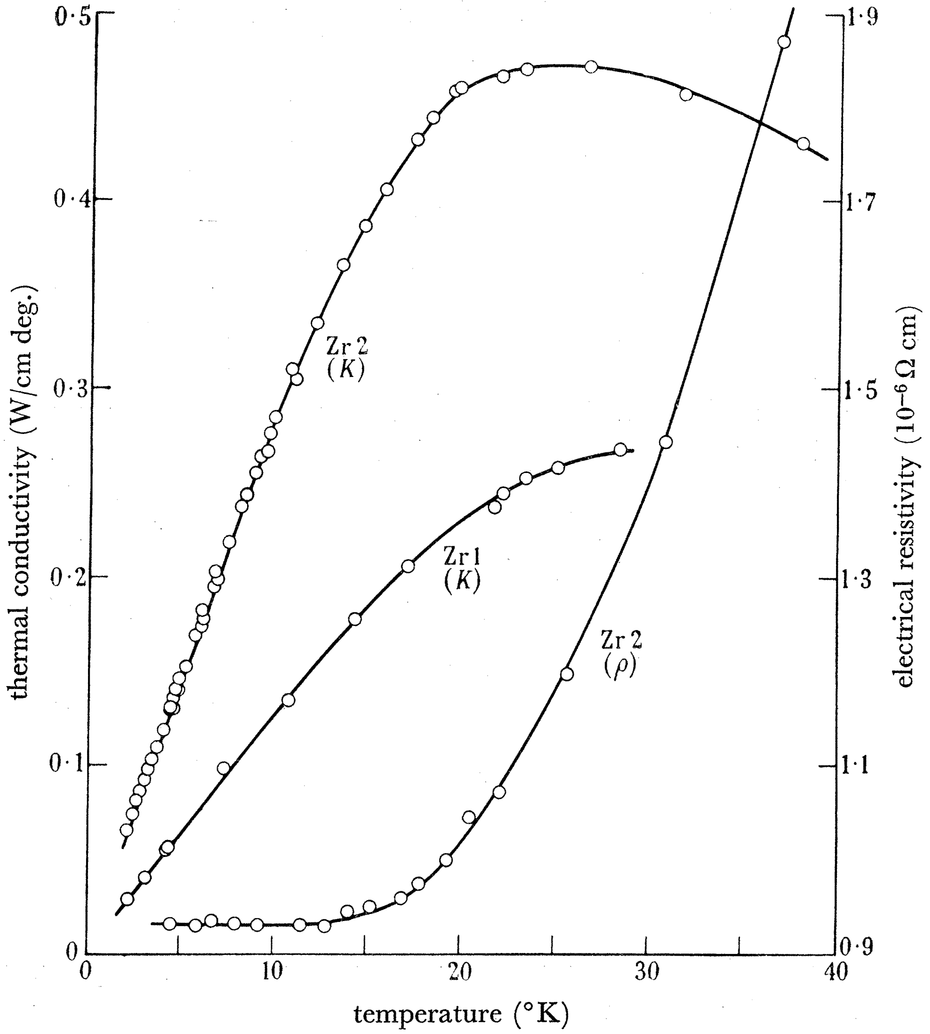

Figure 16. The thermal conductivity K of the zirconium specimens, Zr 1 and Zr 2, and the electrical resistivity, ρ, of Zr 2.

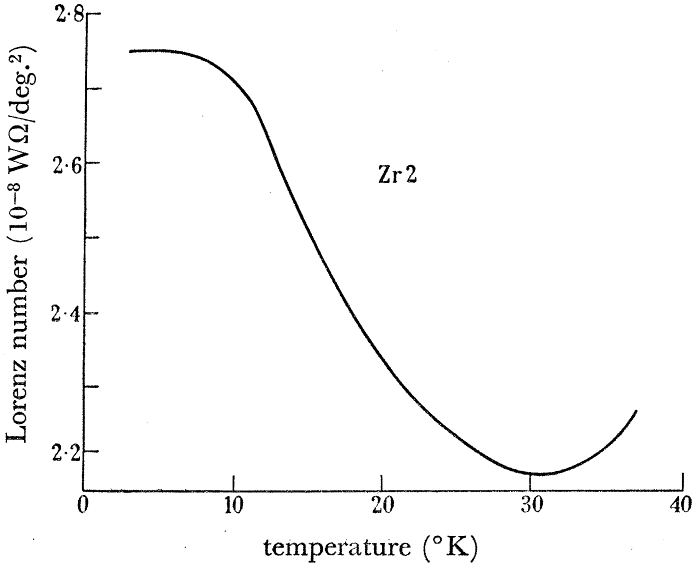

Figure 17. The value of the Lorenz number, L, for Zr 2.

Lead

This single crystal, Pb 1, was made from 99·998 % purity Tadanac lead from Messrs Goodlass Wall and Lead Industries Ltd. The normal and superconducting graphs are shown in figure 20. In the normal state the metal has a very high maximum at about 3° K. On the low-temperature side of this maximum the conductivity was still quite high and was changing very rapidly so that it was not possible to take accurate readings in this region. Hence no experimental point is shown.

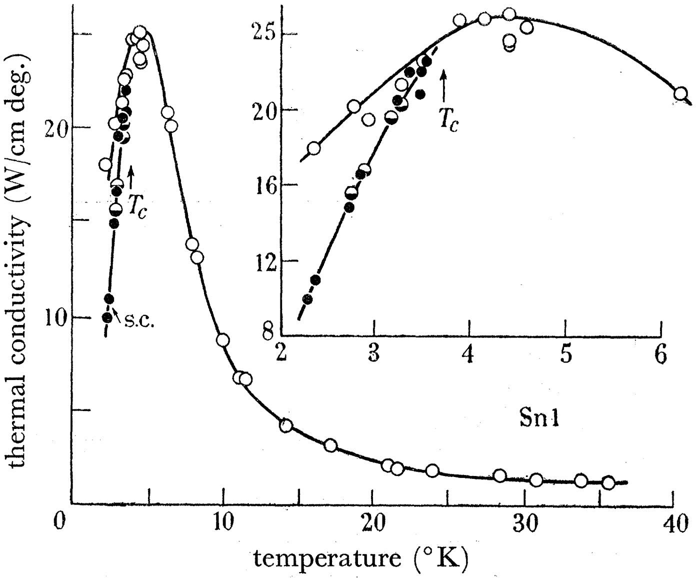

FIGURE 18. The thermal conductivity of the tin single crystal. The inset shows the curve below the superconducting transition temperature, T_c, on a larger scale. Points taken in zero magnetic field are shown as filled circles. Half-filled circles are points taken when the field is again reduced to zero after superconductivity has been destroyed by a magnetic field. These fall on the original superconducting curve showing that there is no frozen-in flux.

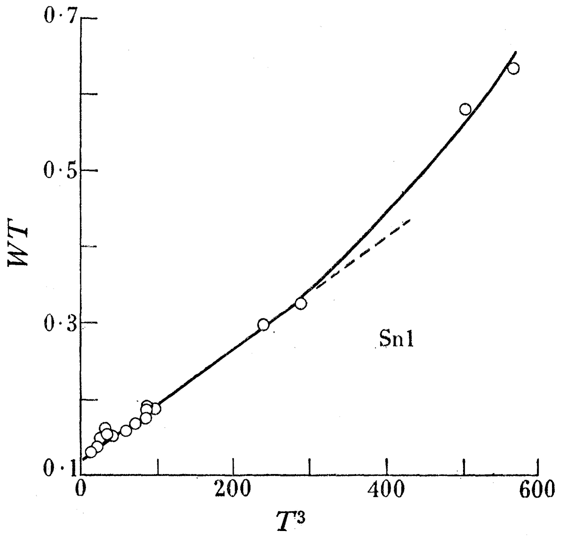

FIGURE 19. The graph of WT against T^3 for the tin single crystal, showing the departure from linearity.

The superconducting curve is interesting in two respects. First, it breaks away from the normal curve with a discontinuous change of slope which is in contrast to the behaviour of tin. Secondly, there is a shallow minimum in the conductivity at about 5° K. Both these effects have been reported by de Haas & Rademakers (1940), and similar behaviour is shown by Hulm's mercury specimen, Hg 3. The rise in the conductivity on the low-temperature side of this minimum may have a connexion with the extremely rapid increase in the normal conductivity in this temperature range. It might, however, be an

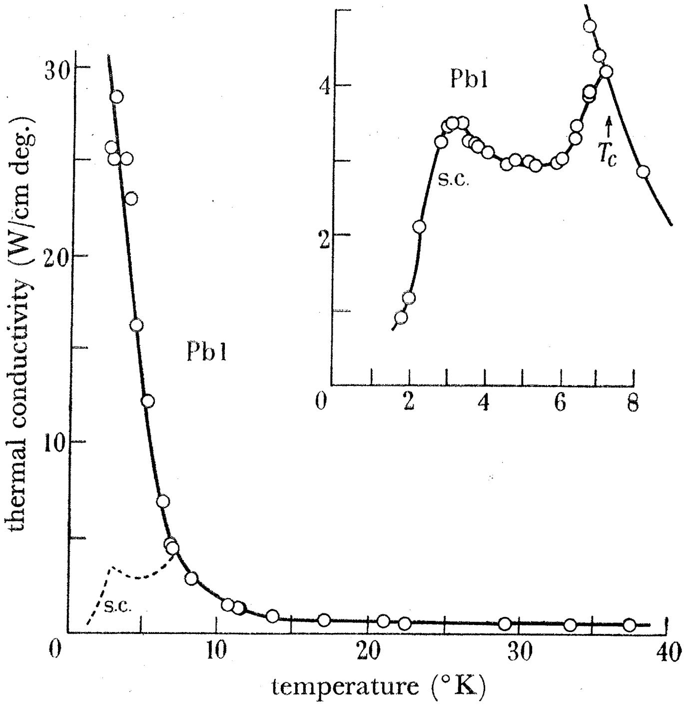

FIGURE 20. The thermal conductivity of the lead single crystal. The inset shows the curve for the superconducting state on a larger scale.

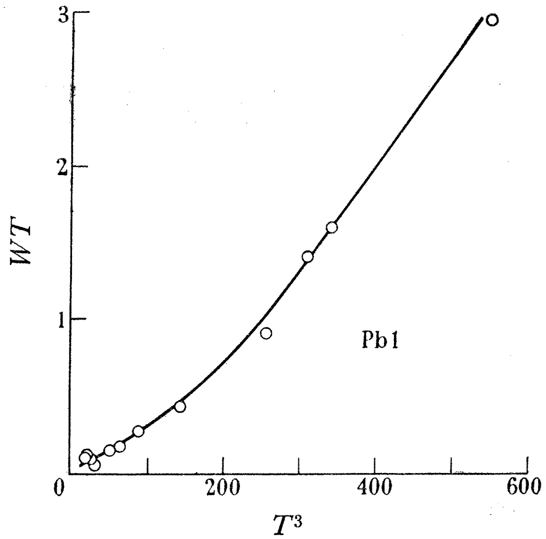

FIGURE 21. The graph of WT against T^3 for the lead single crystal showing the departure from linearity.

indication of the change in the scattering mechanism from lattice scattering to impurity scattering which does occur at these temperatures. A full investigation of the superconducting normal relations in our specimens, however, is outside the scope of the present research. More detailed information is given by Hulm (1950) and Olsen & Rosenberg (1953).

The graph of WT against T^3 (figure 21) is similar to that for Sn 1 in that the slope increases at about 5° K. Similar non-linearity is also shown by the specimen of de Haas & Rademakers (1940). The best value of α from our results is 290×10^{-5} up to 5° K. From de Haas & Rademakers's paper Hulm has calculated $\alpha = 220\times10^{-5}$.

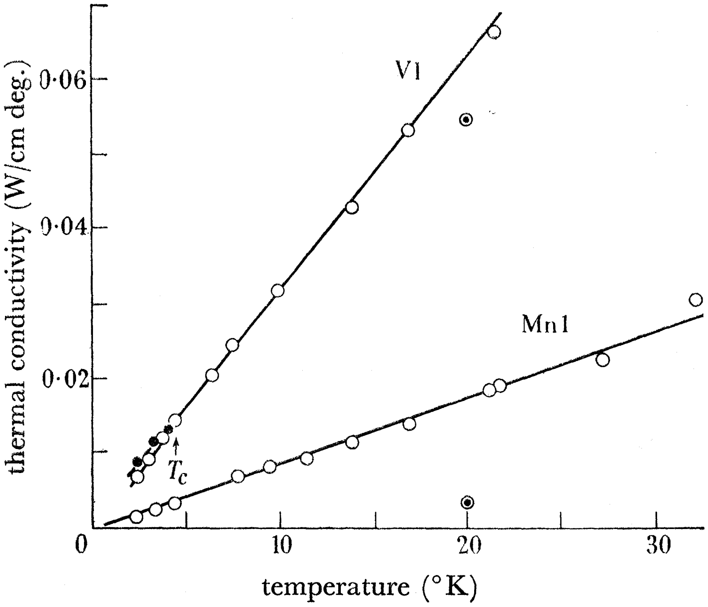

FIGURE 22. The thermal conductivity of the vanadium and manganese specimens. The ringed points show the thermal conductivity as calculated from the electrical resistivity assuming the validity of the Wiedemann–Franz law.

8·8. *The metals of group 5a*

All the metals in this group have been investigated. They are vanadium, columbium and tantalum. Each is a so-called 'hard' superconductor. Their thermal conductivity curves are shown in figures 22 to 25.

Vanadium

This specimen, V 1, was a piece of unannealed wire presented by Johnson, Matthey. It was stated to have been made from spectrographically standardized metal, although the actual purity was not given. At first an attempt was made to anneal the wire, but this entirely altered its physical properties and it became exceedingly brittle and fragile. It was therefore decided to use the unannealed specimen. The thermal conductivity curve, which is the upper one on figure 22, is almost linear above the superconducting transition temperature, 4·3° K. The value of the conductivity is very low and may in part be due to the strained state of the specimen. The production of such a wire is quite a technical achievement, and it is very likely that the crystal lattice is strongly distorted in the manufacture. The superconducting curve shows the usual behaviour of falling below the normal conductivity curve, but the latter, instead of being a continuation of the upper part of the graph, seems to curve very slightly upwards away from the straight line. The

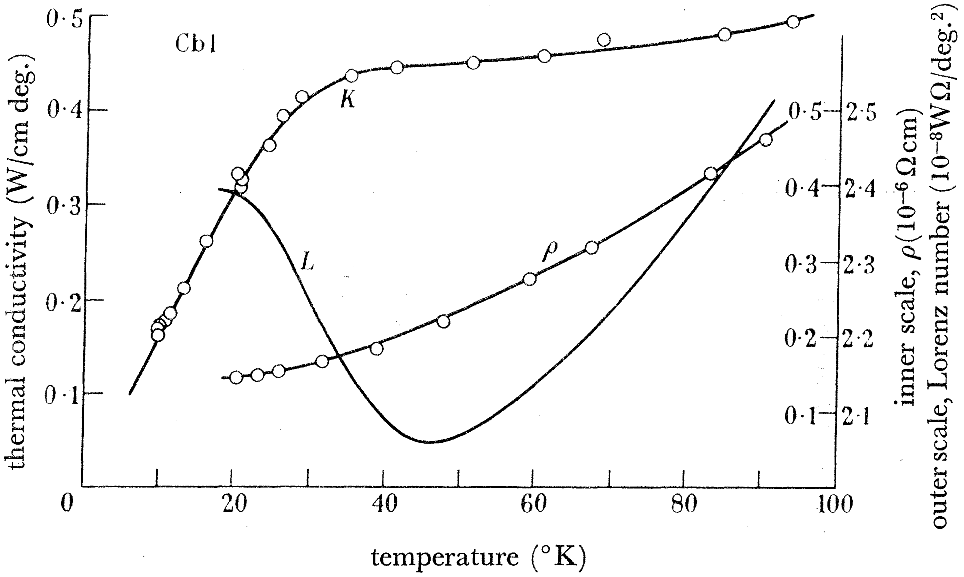

FIGURE 23*a*. The thermal conductivity, K, the electrical resistivity, ρ, and the Lorenz number, L, for the columbium specimen.

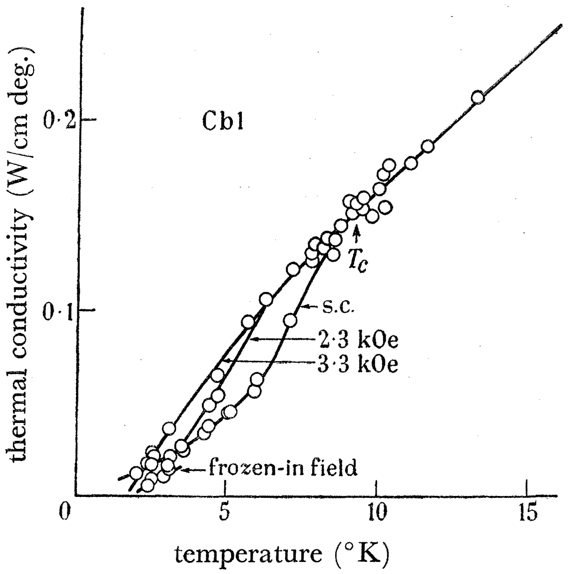

FIGURE 23*b*. The thermal conductivity, K, of the columbium specimen below the superconducting transition temperature, T_c. The curves for fields of 2·3 and 3·3 kOe show that below 6° K the normal state is not attained in these fields.

electrical resistance gives a calculated conductivity point which is again appreciably below the experimental curve, but as was the case with the titanium, it does not seem possible to ascribe this to any lattice conductivity.

The WT against T^3 curve gives a value for α of 124×10^{-5}.

Columbium

Cb 1 was an unannealed rod of polycrystalline JM 4526 which had a purity of 99·99 %. This metal, which has a high superconducting transition temperature, 9·22° K, was primarily investigated for its superconducting properties and for its behaviour as a magnetic field was applied to destroy its superconductivity. The thermal conductivity is shown in figures 23*a* and *b*. Above the transition temperature the curve is linear, and below it the curve in zero magnetic field has the usual shape (figure 23*b*). The points taken in 2·3 and 3·3 kOe fields fall on to the continuation of the linear part of the curve at the higher temperatures, but the 2·3 kOe curve drops below this at about 6° K and the 3·3 kOe curve at a slightly lower temperature. If we assume that the conductivity curve for the normal state is a straight line through the origin, then the temperatures where the curves break away from this line correspond to the temperatures at which the respective magnetic fields just destroy the superconductivity. This means that the transition field for columbium at the lower temperatures is greater than 3·3 kOe. This is in agreement with the observations on the transition field by Cook, Zemansky & Boorse (1950). At the time of these experiments a larger field was not available and the true normal curve could not be investigated to lower temperatures.

It will be noted that at about 3° K the 2·3 kOe curve crosses the superconducting state curve so that the conductivity in the transition region is less than that in the superconducting state. This confirms the behaviour first observed by Mendelssohn & Olsen (1950*a*, *b*, *c*) and Olsen (1952) in lead-bismuth alloys and in columbium. Several explanations for this phenomenon have been advanced. Mendelssohn & Olsen have suggested that a circulation flow of superconductive and normal electrons, analogous to the circulation flow of liquid helium II, might account for the thermal conductivity in the superconducting state. This would be inhibited by the application of a magnetic field, and hence the thermal conductivity would decrease initially until the magnetic field had destroyed the superconductivity to such an extent that the production of normal electrons, and the extra conductivity which they would give, was sufficient to make up for this decrease.

Another possible explanation is that the boundaries of the normal and superconducting laminae which are formed in the intermediate state might scatter the electrons strongly and hence produce a decrease in the thermal conductivity. Other suggestions are based on the assumption that in the superconducting state the lattice conductivity is greatly increased, since the lattice waves might not be scattered by the superconducting electrons. The production of normal superconducting boundaries will scatter these lattice waves and hence decrease their conductivity. This will continue until a sufficient amount of the metal is in the normal state whose electronic conductivity will cancel out the decrease in the lattice conductivity. At the present moment it is not possible to decide which of these explanations is correct, although it has been shown (Olsen & Renton 1952; Mendelssohn & Renton 1953) that below 1° K the thermal conductivity in the superconducting state is almost certainly due to lattice conduction.

The lowest curve on the graph shows points taken after the field had been increased to its maximum value and had then been reduced to zero. These do not fall on to the original zero field curve and show that there is a marked frozen-in effect.

The thermal and electrical conductivities up to 90° K are shown in figure 23*a*. The curve of the Lorenz number, L, is also drawn. It will be noted that there is no maximum in the thermal conductivity, presumably because the specimen was too impure. Nevertheless, the curve for L does not give any reason to suggest that there is any lattice conduction present.

The value of α was found to be 50×10^{-5}.

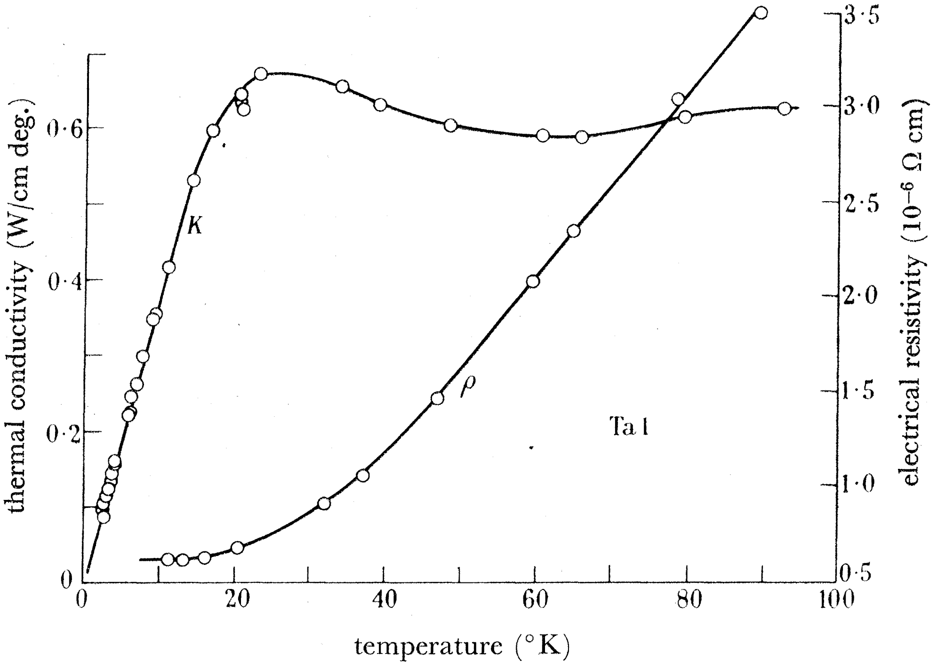

FIGURE 24. The thermal conductivity, K, and the electrical resistivity, ρ, of the tantalum specimen.

Tantalum

This specimen, Ta 1 was an unannealed rod of JM 3804 which had a purity of 99·98 %. Detailed points were taken below the superconducting temperature, 4·38° K, as are shown in figure 25. The rest of the curve up to 90° K, together with the electrical resistivity, is shown in figure 24, and the temperature variation of the Lorenz number, L, is shown in figure 26. As with the other metals in this group the conductivity is not very large, although it is the highest of the three. It has a slight maximum at about 25° K, and this is followed by a very shallow minimum at 60° K. This is the only minimum in the thermal conductivity that has been found in this work. It might be thought that the increase in conductivity above the minimum was only apparent, and was really due to radiation losses as the temperature was increased. This does not seem possible, however, as the maximum radiation loss at 90° K was only 1 %, whereas the conductivity curve at 90° K rises 5 % above its minimum value. The curve for L (figure 26) shows the usual behaviour to be expected for a fairly pure metal. At both high and low temperatures it flattens off to approximately the theoretical value of $2{\cdot}45 \times 10^{-8}$, and in between it decreases and passes through a minimum.

The value of α is 79×10^{-5}.

8·9. *The metals of group 5b*

Antimony

The only metal of group 5*b* which was investigated was antimony. The specimen, Sb 1, was a polycrystalline piece of JM extruded wire which had been annealed *in vacuo* at 500° C for 2 h. The purity was not given, but it was made from spectrographically standardized metal.

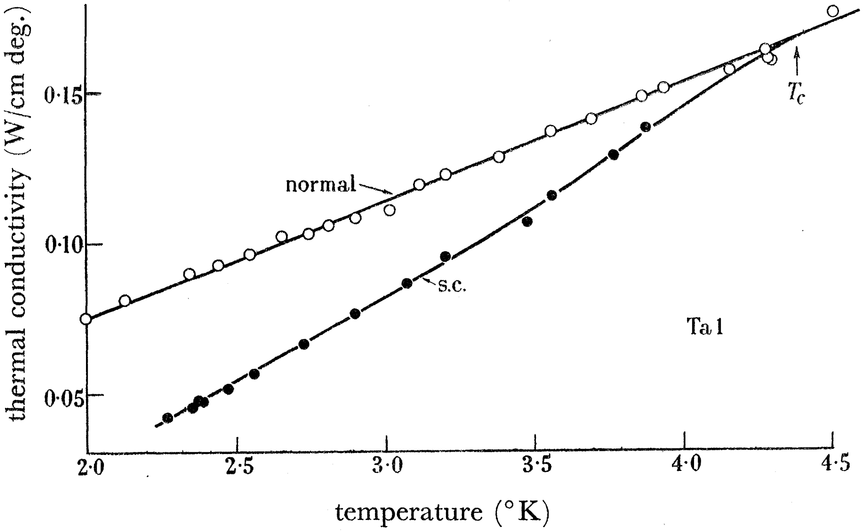

FIGURE 25. The thermal conductivity of the tantalum specimen below the superconducting transition temperature, T_c.

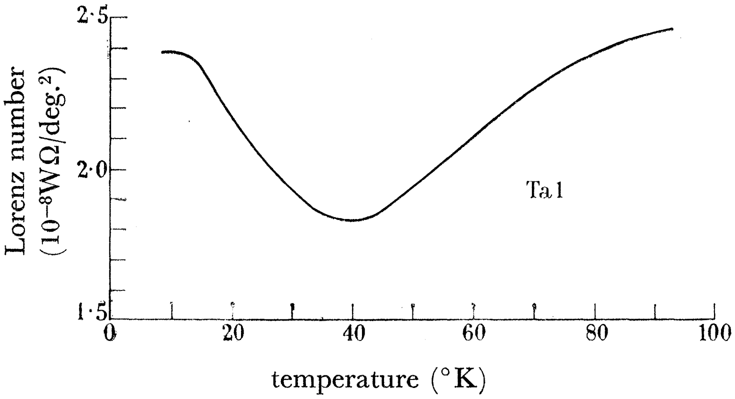

FIGURE 26. The graph of the Lorenz number, L, for the tantalum specimen.

The conductivity curve shown in figure 27 is unlike any other that is presented in this research, since it indicates a large lattice conductivity in the specimen. This is at once evident by the fact that at low temperatures the curve is not linear through the origin, as in the other metals, but is proportional to a higher power of T. Electrical resistance measurements at hydrogen temperatures give a low electronic thermal conductivity as is shown in the graph. This has been subtracted from the total conductivity to give the lattice contribution, which is also drawn. A logarithmic plot of the lattice conductivity, K_g, against temperature indicates that up to about 6° K, K_g is proportional to $T^{2 \cdot 3}$. This is very near to the theoretical dependence of K_g on T when K_g is limited by electron scattering. The theory gives K_g as proportional to T^2 (Makinson 1938). This fairly high lattice conductivity of antimony is to be expected, since the number of free electrons is known to be very small and hence the lattice waves are not scattered to too great an extent. Other pure metals which show a similar behaviour are bismuth (Olsen 1951) and a tellurium specimen which has been investigated. The results for this latter specimen have not been presented in detail since, owing to experimental difficulties, it was not possible to obtain accurate results. Nevertheless, the rough graph which was obtained is very similar in shape to that of Sb 1 and it also shows a proportionality to T^2, approximately.

It will be noted that none of these metals, antimony, bismuth or tellurium, can be regarded as having very metallic properties, and hence it is not surprising that their thermal conductivities should also differ in behaviour from the other metals which we describe.

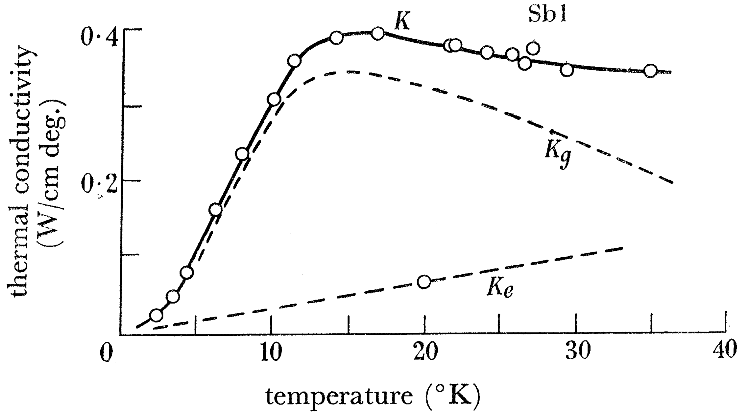

FIGURE 27. The thermal conductivity of the antimony specimen. This shows the total conductivity, K, the electronic contribution, K_e, and the lattice conductivity, K_g.

The K_g curve shows a maximum, since the lattice waves are also scattered by impurities and dislocations and this resistance is proportional to T^{-1}. Hence at higher temperatures this becomes the dominant scattering mechanism and thus the conductivity is reduced once more.

8·10. *The metals of group 6a*

Molybdenum and tungsten were investigated in this group and their thermal conductivities are shown in figure 28. Although chromium of sufficient purity was available, it could only be obtained in the form of thin brittle flakes which cannot be used for these experiments.

Molybdenum

The specimen, Mo 1, was an unannealed polycrystalline rod of JM 2331 which had a purity of 99·95 %. Both its thermal and electrical conductivities were measured up to 90° K. These are both shown in figure 28 together with the curve for the Lorenz number, L. This shows the characteristic minimum at intermediate temperatures, and it tends to the theoretical value, L_0, in the liquid-hydrogen region.

The value of α was found to be $7{\cdot}5 \times 10^{-5}$.

Tungsten

W 1 was a polycrystalline rod of JM 2260 which had been annealed *in vacuo* for several hours at 1150° C. Its purity was 99·99 %.

The conductivity curve is very similar to that for Mo 1. This is to be expected, since they both have similar crystal structures and values of Debye temperature.

It is interesting to compare the maximum conductivity of our tungsten specimen with that of a single crystal of the metal which was investigated at hydrogen temperatures by de Haas & de Nobel (1938). Their specimen had a maximum conductivity of about 75 W units at 15° K, whereas our W 1 has its maximum of 3·5 W units at about 30° K. The influence of the single-crystal structure is thus seen to be very strong.

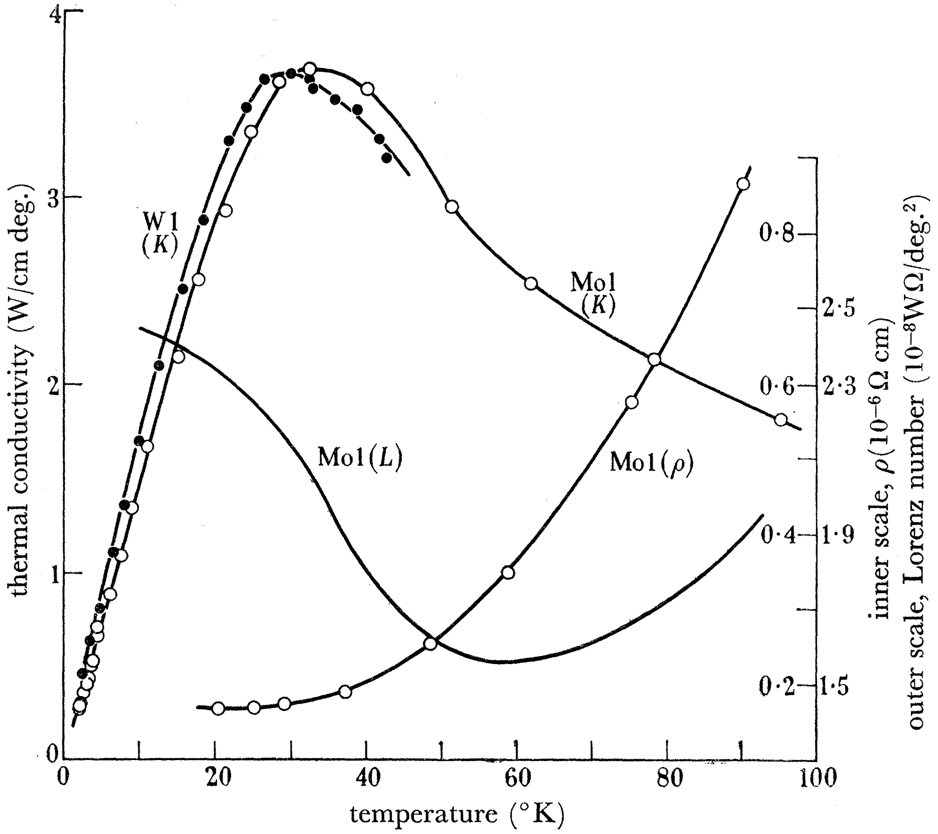

FIGURE 28. The thermal conductivity (filled circles) of the tungsten specimen and the thermal conductivity (K), the electrical resistivity (ρ) and the Lorenz number (L) of the molybdenum specimen.

The value of α which has been calculated from the WT curve is $9{\cdot}3 \times 10^{-5}$. This value compares quite well with that of $8{\cdot}8 \times 10^{-5}$ calculated by Hulm (1950) from some early work by de Haas & Bremmer (1936).

8·11. *The metals of group 7a*

Manganese

This was the only metal in group 7*a* which was available in a suitable form for thermal conductivity measurements. The specimen was electrolytic manganese cut from polycrystalline JM 2472 which had been annealed *in vacuo* for several hours. It had a purity of 99·99 %.

The conductivity curve, which is the lower one in figure 22, shows that the specimen had a very low conductivity, the smallest that was measured in these experiments. The curve is linear and hence no value of α could be calculated. The electrical resistance point shown is very much below the conductivity curve, but, as has been explained previously, it is unlikely that this is due to the presence of a large lattice conductivity K_g, since if it was, K_g would have to be proportional to T and this does not seem to be possible.

While the very small conductivity seems to be due to 'impurity' scattering, it is possible that the impurity in this case is partly due to the extremely complicated crystal structure of manganese.

8·12. *The metals of group* 8

The 3*d* transition group

All the metals of the 3*d* group were investigated and their conductivities are shown in figures 29 and 32.

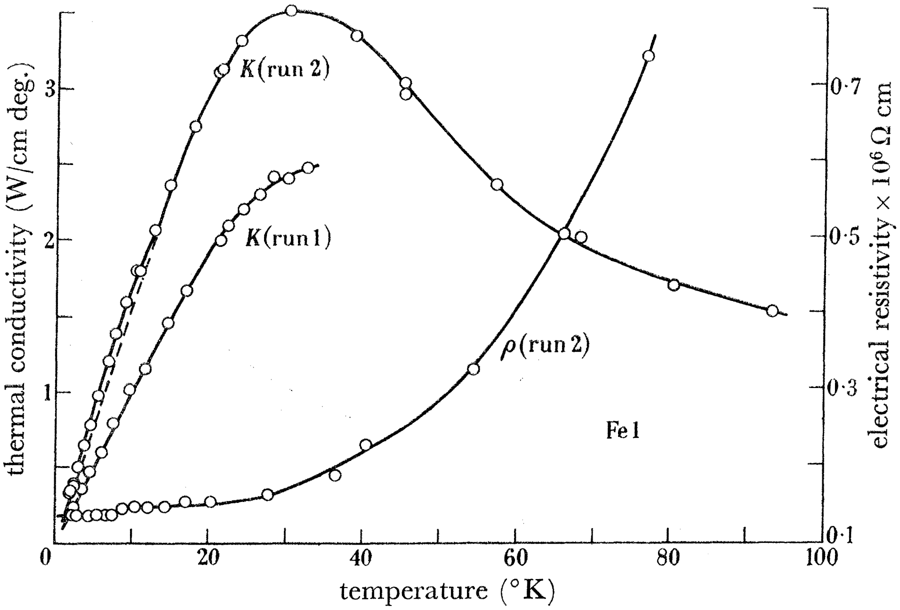

FIGURE 29. The thermal conductivity (K) and the electrical resistivity (ρ) of the iron specimen. This shows the change in K between the two runs during which time it is assumed the precipitation of impurities took place.

Iron

This specimen, Fe 1, was a rod of polycrystalline JM 4975 which had been annealed *in vacuo* for several hours. Its purity was 99·99 %. Two experimental runs were done on this specimen. The first in the range up to 32° K showed that the maximum had not yet been reached, and it was decided, after the technique for measurement at higher temperatures had been improved, to measure the conductivity from 30 to 90° K. This experiment was done about two years after the first run, and it was noted that the curves for the two experiments did not join up, the later experiment giving results that were about 50 % higher than the earlier one. It was therefore decided to do a complete new determination of both the electrical and thermal conductivities down to 2° K, and these are shown in figure 29, together with those of run 1. The electrical conductivity of the specimen at 20° K had increased 1·52 times between the two runs, which is almost the same as the increase of 1·58 for the thermal conductivity. Hence there was no question that the earlier thermal conductivity measurements were wrong. The room-temperature electrical resistance had not changed at all, showing that the form factor had not altered due to corrosion of the metal in the interval between the two runs.

From the WT curves the value of α came out to be approximately the same for both runs, α being $10{\cdot}2\times10^{-5}$ for the first and $9{\cdot}5\times10^{-5}$ for the second. The change in the conductivity that was observed was at first sight rather surprising. A decrease might have been explained as being due to damage to the specimen between the two runs, but it could not account for an increase. The increase can be explained as being due to the precipitation of impurity atoms from solid solution with the iron. These impurities would probably be carbon or nitrogen or possibly oxygen or hydrogen.* Experiments by Wert (1950), in which he allowed iron with carefully controlled amounts of impurity to age harden at room temperature, showed that their electrical resistance at liquid-air temperature decreased with time.† This was ascribed to precipitation of the impurity. An analysis‡ of our specimen gave the following impurities: oxygen 0·21 %, carbon 0·01 %, nitrogen and hydrogen not detected. It thus seems very likely, therefore, that precipitation of oxygen or carbon had occurred between runs 1 and 2.

The decrease in the resistance can be qualitatively understood by assuming that the precipitation decreases the number of impurity scattering centres in the metal. Hence the mean free path of the electrons is increased, and this will result in a reduction in both the thermal and electrical resistivities.

Another interesting point arises when the thermal conductivity points of run 2 are examined more carefully. The low-temperature section of the curve is not quite linear. It has a slight curvature so that it lies above the straight line through the origin (run 1 shows this curvature to a smaller extent). This strongly resembles the curve that was obtained for magnesium, and as for Mg 2, it appears to be connected with an anomaly in the residual electrical resistance. In this case, however, no minimum was detected, but a sharp, though not discontinuous, drop in the electrical resistance was found at about 8° K. The change amounted to about 10 % of the resistance and it is shown in the figure. Figures 30 and 31 show corresponding anomalies in both the WT-T^3 curve and in the temperature dependence of the Lorenz number, L. The points for WT fall below the linear part of the curve at 12° K and then gradually return to it. The curve for L is of the characteristic shape for a pure metal, except that at the low-temperature end, before it flattens off to a constant value it rises to a sharp peak, the temperature at which this occurs corresponding to that of the decrease in the electrical resistance. It thus appears that the thermal conductivity does not change as much as the electrical resistance at this point.

Cobalt

Co 1 was a polycrystalline rod of spectrographically standardized metal presented by Johnson, Matthey. The purity was not given. It was annealed *in vacuo* for several hours.

---

* I am extremely grateful to Professor A. H. Cottrell who first made this suggestion to me.

† This problem has been treated theoretically by Bhatia (1949).

‡ I should like to thank Mr M. Mapper of the Atomic Energy Research Establishment, Harwell, for very kindly making this analysis.

The conductivity (fig. 32) is of a similar order of magnitude to that of Fe 1. The electrical resistance points of Co 1 and of the nickel specimen gave a calculated thermal conductivity which is in good agreement with the continuation of the linear part of the experimental curves. The value of α is $10{\cdot}5\times10^{-5}$.

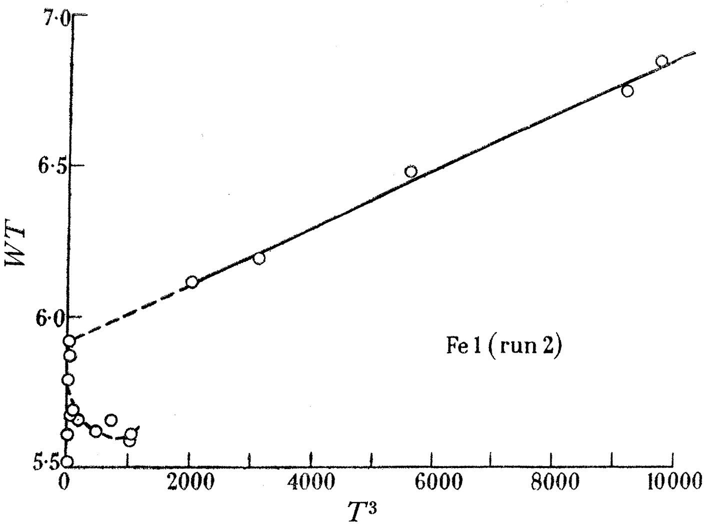

FIGURE 30. The graph of WT against T^3 for the iron specimen.

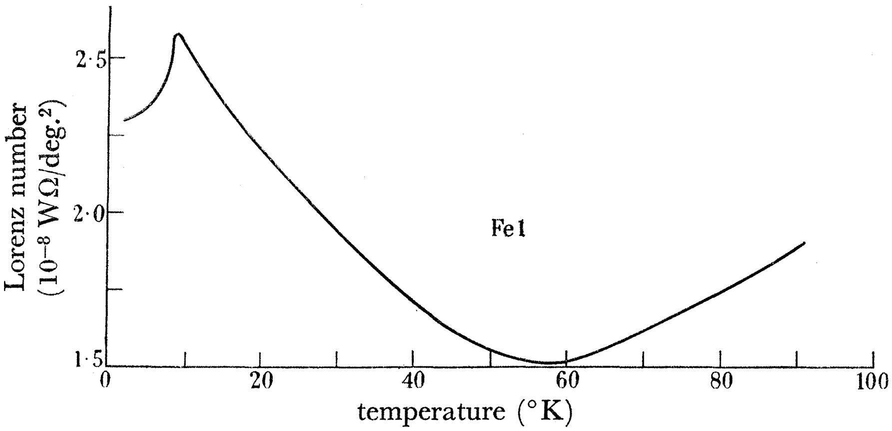

FIGURE 31. The value of the Lorenz number for the iron specimen.

Nickel

This specimen, Ni 1, was a polycrystalline rod of JM 4884 which had been annealed at 1150° C for several hours *in vacuo*. It had a purity of 99·997 %. The thermal conductivity curve (figure 32) is the highest of the metals in this group, the maximum being nearly 4 W units. The value of α which has been calculated is $10{\cdot}4\times10^{-5}$.

It will be noted that for each of these three transition metals α has approximately the same value: 10·2 and 9·5, 10·5 and $10{\cdot}4\times10^{-5}$ for iron, cobalt and nickel respectively. This correspondence has not been found for the metals in the other group 8 series. This is in part due to the fact that only in the 3*d* group are the Debye temperatures approximately the same for the three metals.

The 4*d* transition group

In this group we have investigated rhodium and palladium. The thermal conductivity curves are shown in figure 33.

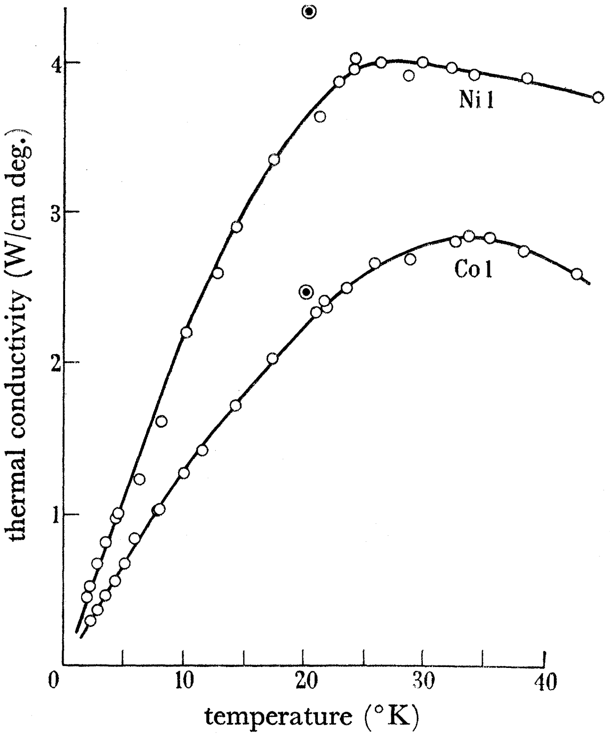

FIGURE 32. The thermal conductivity of the specimens of cobalt and nickel. The ringed points are the thermal conductivities as calculated from the electrical resistivities assuming the validity of the Wiedemann–Franz law.

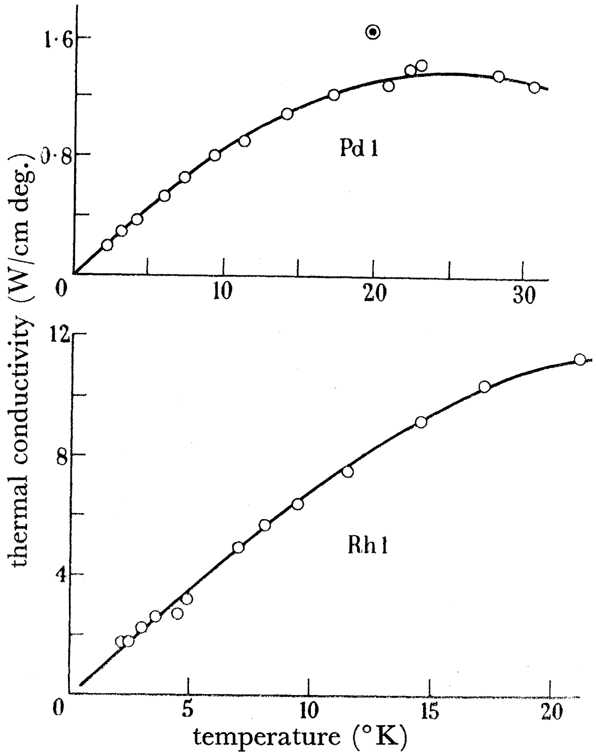

FIGURE 33. The thermal conductivity of palladium and rhodium. The ringed point shows the thermal conductivity of palladium as calculated from the electrical resistivity assuming the validity of the Wiedemann–Franz law.

Rhodium

This specimen, Rh1, was made from unannealed wire, JM2357, which had a purity of 99·995 %. The lower curve in figure 33 shows that it had quite a high conductivity which rose to about 11 W units in the temperature range covered. This was one of the earlier experiments, and it was not possible to extend the measurements to higher temperatures so as to reach the region of the conductivity maximum.

The WT curve for this specimen is not very linear for a specimen which has a Debye temperature of 370° K. It bends over towards T^3 axis at about 11° K, which is much lower than one would expect. The best value for α up to this temperature is $10{\cdot}7\times10^{-5}$.

Palladium

Pd1 was a polycrystalline rod of JM2134 which had been annealed *in vacuo* at 1150° C for several hours. Its purity was 99·995 %. The conductivity which is shown in the upper graph of figure 33 is only 10 % of that of the rhodium at any given temperature and it has a maximum at about 25° K. The electrical resistance point falls on the continuation of the linear part of the curve. As for Rh1, the WT curves are not very linear, and it was difficult to get a good value of α to cover the full range of temperature. 41×10^{-5} seems to be the most representative value.

The 5*d* transition group

Iridium and platinum have been investigated in this group. It was not possible to obtain osmium in a form suitable for thermal conductivity determination. The curves are shown in figure 34.

Iridium

Ir1 was a polycrystalline wire of JM3441 which had been annealed *in vacuo* at 1150° C for several hours. It had a purity of 99·995 %. The thermal conductivity is the highest measured in this research among the transition metals, having a maximum of about 18 W units at 20° K. In this case the WT curves bend away from the T^3 axis, but up to 27° K the value of α is approximately $4{\cdot}6\times10^{-5}$. The electrical resistance point is too high to plot in the figure, but it confirms the experimental curve.

Platinum

This specimen, Pt1, was a polycrystalline wire of JM2157*b* which had been annealed *in vacuo* for several hours. The purity was given as 99·999 %. The conductivity curve in figure 34 does not show such a high maximum as does Ir1, but it is sharper and is shifted to a lower temperature. This is probably due to the lower Debye temperature of platinum. While there is a slight initial curvature to the WT curve it is otherwise quite linear up to 17° K, and this gives a value for α of 43×10^{-5}.

The general picture given by the experiments on the transition elements of group 8 is similar to that of the other metals in the general shape of the curves. There does seem to be a greater tendency, however, for the plots of WT against T^3 to be more irregular, particularly in the 4*d* and 5*d* groups, than for the other metals. Nevertheless, considering that the theory relates to a simple monovalent model of a metal, it is hardly surprising that the transition metals do not fit very closely to the theoretical predictions.

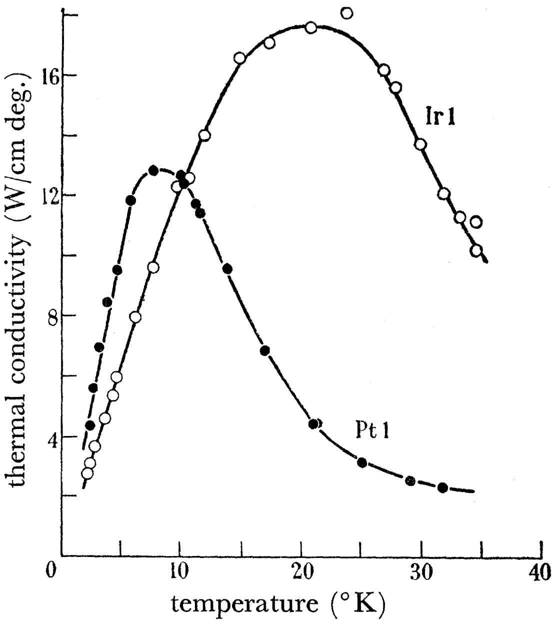

FIGURE 34. The thermal conductivity of the specimens of iridium and platinum.

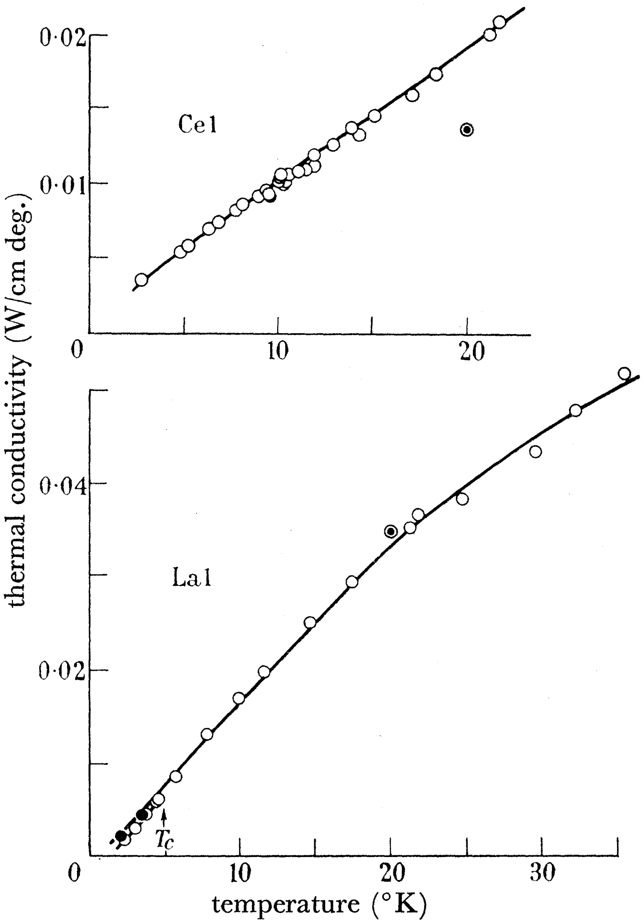

FIGURE 35. The thermal conductivity of the lanthanum and cerium specimens. The ringed points show the thermal conductivity as calculated from the electrical resistivity assuming the validity of the Wiedemann–Franz law.

8·13. *The rare-earth metals*

While it was not possible to obtain or take measurements on many of the metals of the rare-earth group, some idea of the general behaviour of the group was obtained by investigating the thermal conductivity of lanthanum and cerium. Their conductivity curves are shown in figure 35. Both have a very low conductivity.

Lanthanum

La 1 was obtained from Professor Spedding of Iowa State University. It was a small block of polycrystalline, unannealed metal. Its purity was better than 99·94 %, the largest impurities being calcium and beryllium. As can be seen from the graph, the conductivity is only of the order of 10^{-2} W unit. The metal becomes superconducting in zero magnetic field at about 4·7° K. Below this temperature some measurements were taken in a 3·3 kOe field, as well as in zero field, in an attempt to measure the thermal conductivity in the normal state. These points, however, are not linear through the origin, and at first sight it might be thought that this was due to an appreciable lattice conductivity being present. The electrical resistance point at 20° K shows that this is not the case, since it falls exactly on the extrapolation of the linear section of the experimental curve. The most obvious explanation, therefore, is that the 3·3 kOe field was not sufficient to destroy the superconductivity completely and that the metal was, in fact, in the transition region in this field.

Cerium

Ce 1 was also obtained from Professor Spedding and was in a similar form to the lanthanum. The purity was stated to be 99·6 %, the greatest impurities being magnesium and calcium. The thermal conductivity curve, shown as the upper graph in figure 35, is linear over the range measured, and the conductivity is about one-half that of La 1. The electrical resistance point at 20° K is well below the experimental curve, and this was thought to be good evidence that this specimen had a measurable lattice conductivity. Again we are faced with having to explain the existence of a linear lattice conductivity, a very unlikely occurrence. The only other possibility seemed to be that for this metal the Wiedemann–Franz law did not hold at liquid-hydrogen temperatures. Recent work by James, Levgold & Spedding (1952) seems to bear this out. They measured the electrical resistivity of cerium from 2·2 to 300° K, and two points of interest have been found. First, the region of residual electrical resistance was not reached at 20° K, and even at liquid-helium temperatures the resistance was still decreasing. Secondly, the electrical resistivity in this range did not follow a smooth curve. At 14° K there was an anomaly in the curve where the resistance fell much more rapidly as the temperature was lowered. Under such circumstances it is quite likely that the Wiedemann–Franz law is invalid at 20° K, and hence it is not surprising that our electrical resistance point does not agree with the experimental curve. No anomaly corresponding to that found in the electrical resistivity was detected in the thermal measurements.

It is thus possible that the behaviour of such specimems as vanadium and manganese, which also had a linear conductivity and whose electrical resistance point fell below the experimental curve, might also be explained by a failure of the Wiedemann–Franz law. In fact the more detailed investigations into the electrical conductivity of Ti 3 and Zr 2, which have already been mentioned, show that the value of the Lorenz constant for these metals is higher than the theoretical value. It seems difficult to ascribe the deviations to errors in measurement, because in these cases the thermal and electrical conductivities are so small that it is a comparatively simple matter to determine them accurately.

8·14. *Uranium*

This metal does not fit conveniently into any other group, and it is thus dealt with separately. The specimen was an unannealed rod from the Atomic Energy Research Establishment, Harwell. Its purity has not been given, but it is believed to be very high. The thermal and electrical conductivities were measured up to 90° K and they are shown in figure 36. The thermal conductivity is increasing throughout the range although even at 90° K it was only 0·27 W, and in the liquid-helium region it was very low indeed. A curious feature is the way the conductivity starts to increase more rapidly at about 60° K. The Lorenz number, L (figure 37), at this temperature rises above its theoretical value and continues to increase up to 90° K. It appears likely that in this region there was some lattice conductivity. Using the values of the electrical resistance, the electronic thermal conductivity, K_e, has been calculated between 60 and 90° K, and this is shown by a dotted line on the graph. It can be seen that it runs fairly smoothly into the lower curve and it has a more or less constant value. The difference between this and the experimental curve gives the lattice conductivity, K_g, and this has also been drawn in the figure. It increases quite rapidly with the temperature. Owing to the fact that the lower part of the experimental range is that in which L would not be expected to have the value L_0, it is not possible to ascertain whether there is any lattice conductivity at the lowest temperatures.

It is interesting to note that measurements of the expansion coefficient of uranium by Bijl & Pullan (1955) show that it has a value of zero in the region of 60° K, being positive above this temperature and negative below. Thus from a thermal expansion point of view the lattice starts behaving like a normal crystal at 60° K. This is just the temperature at which our specimen starts to show a lattice conductivity. It is too early to state whether there is in reality any connexion between the cause of the two effects, but the fact that they both start at the same temperature suggests that there might be.

Tyler, Wilson & Wolga (1952) have measured the thermal and electrical conductivities of uranium from 20 to 300° K. Their sample had a heat conductivity at 20° K, which was about 70 % of that of our specimen. They, too, showed that the Lorenz number was greater than L_0 for temperatures above 60° K, but they made no estimate of the lattice conductivity.

From WT plots it was difficult to get a good value of α over the entire temperature range as the curve bends over at 13° K. Up to this temperature, however, the best value seems to be $\alpha = 790 \times 10^{-5}$.

9. Discussion and summary

In a series of experiments such as have been described it is clearly not possible to correlate all the results obtained or to draw detailed conclusions from all of them. Indeed, as has already been remarked, the primary object of this work has been the collection of data. A detailed theoretical discussion on the results is therefore not presented, but, nevertheless, they do emphasize some points which it is considered are of interest. These are dealt with in this section.

The experiments show that for all pure metals, except those such as antimony and bismuth, which are already recognized as not having full metallic properties, the heat transport is due almost entirely to electronic conduction. The amount of heat transported by the lattice is negligible. At low temperatures the dependence of the thermal resistance, W, on the temperature is well represented by the relation $W = \alpha T^2 + \beta/T$, although in some cases this equation breaks down at a lower temperature than one would expect from a knowledge of the theory as developed by Wilson, Makinson, Sondheimer, etc. Most pure metals exhibit a maximum in the thermal conductivity in the region 2 to 40° K. The higher the value of the Debye temperature of the metal, the broader is this

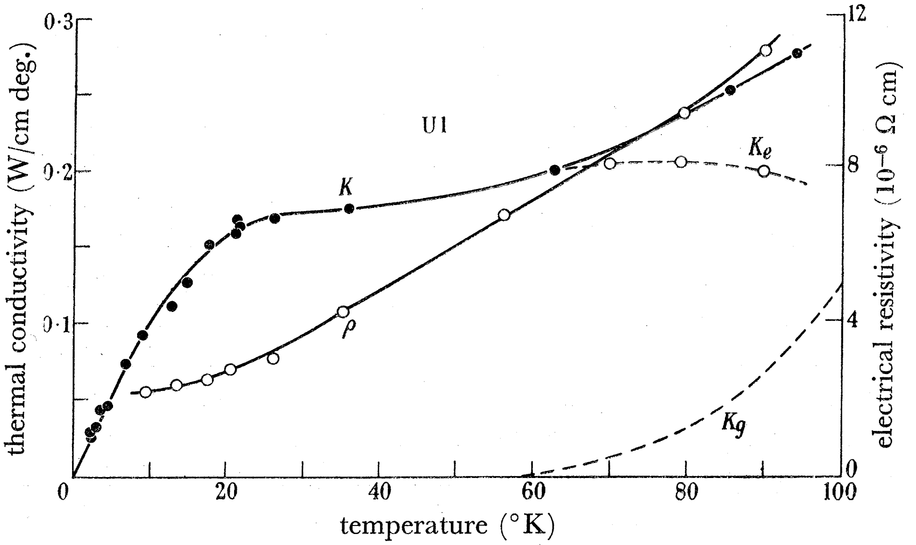

FIGURE 36. The thermal conductivity (K) and the electrical resistivity (ρ) for the uranium specimen. The electronic contribution to the thermal conductivity (K_e) and the lattice conductivity (K_g) are shown by dotted lines.

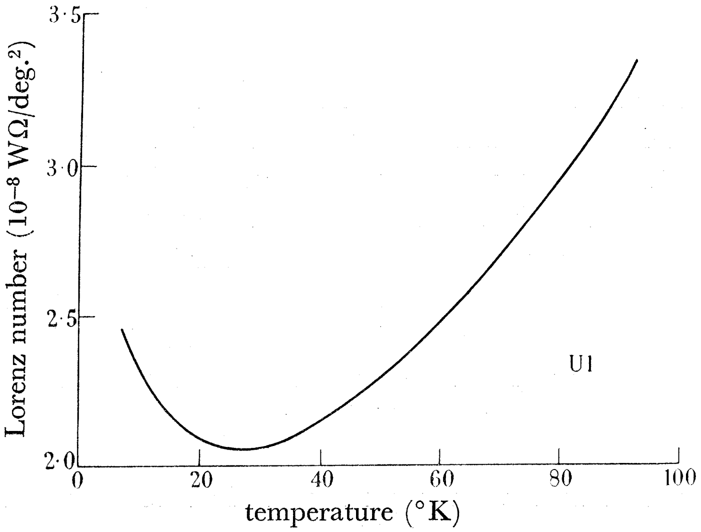

FIGURE 37. The value of the Lorenz number for the uranium specimen.

maximum and the higher the temperature at which it occurs. For a purer specimen of the same metal, the maximum has a larger value; it is sharper and it occurs at a lower temperature. For those specimens where the experimental range extended some way to the high-temperature side of the maximum, no indication of a minimum in the conductivity was found (except in the tantalum specimen).

For metals which are superconductors the thermal conductivity is less in the superconducting state than in the normal state. In most cases there is no discontinuous change of slope at the superconducting transition temperature between the curve above this temperature and the superconducting curve. The only exception to this was the lead specimen. It has been suggested by Hulm (1950) that behaviour such as is exhibited by lead occurs only if the superconducting transition temperature is to the high-temperature side of the maximum in the normal conductivity, i.e. where scattering by the lattice waves is dominant.

TABLE 3

group 1*b*	$10^5\alpha$	group 2*b*	$10^5\alpha$	group 3*b*	$10^5\alpha$
Cu	2·5	Zn	32	Ga	23 to 160
Ag	5	Cd	122	In	185
Au	19			Tl	537

When the metals are considered in their groups in the periodic classification of the elements, the conductivity of the metals in one group, as is to be expected, is very similar. The value of the lattice scattering coefficient, α, increases for higher atomic number in any given group. This is shown in table 3 for groups 1*b*, 2*b* and 3*b*.

If the complete sets of transition metals are compared and not just the elements of group 8, then it is seen that the lighter members of each of the 3*d*, 4*d* and 5*d* groups have a much lower conductivity than those which occur in group 8.

TABLE 4

group 1*b*	$K_\infty\theta^2\alpha$	group 2*b*	$K_\infty\theta^2\alpha$	group 3*b*	$K_\infty\theta^2\alpha$	group 4*b*	$K_\infty\theta^2\alpha$
Cu	10·2	Zn	31·3	In	20·3	Sn	12·8
Ag	11·1	Cd	34·7	Tl	21·7	Pb	11·2
Au	16·1						

There did not seem to be any point in calculating from the equation (8) the value for the effective number of electrons per atom, N_a, since the figure which is obtained is known to be very much lower than what one would expect from metallic theory or from other types of experiment. As has been mentioned in § 7, Ziman (1954) has shown that this discrepancy is due to the fact that *U*-processes were not considered in the earlier calculations. Nevertheless, it seemed of interest to calculate the value of $K_\infty\theta^2\alpha$ for the metals of each group. According to equation (8) this expression should be equal to constant $\times N_a^{2/3}$, and even if this is not correct it should be a function of N_a. Since N_a might be expected to be very similar for all the members of one group, the comparison of the values obtained from each group was of interest. These are shown in table 4, and it can be seen that within each group the expression $K_\infty\theta^2\alpha$ is approximately constant. It was not possible to determine this for every metal, as the value of K_∞ is not available in every case. The specific heat θ has been used in these calculations.

It thus appears that $K_\infty \theta^2 \alpha$ can be considered as a kind of normalizing factor for the metals of a given group. It should be noted that the values for each group given in table 4 are not proportional to $N_a^{2/3}$ when N_a is equal to the valency of the group. There is thus no simple connexion between the values for the different groups. In fact, since it is generally agreed that the effective value of N_a for the higher groups is less than the valency number it is surprising* that the figures in table 4 for group 2*b* are about three times higher than those for group 1*b*. This seems to indicate that the constant in equation (8) is greater for group 2*b* than for group 1*b*.

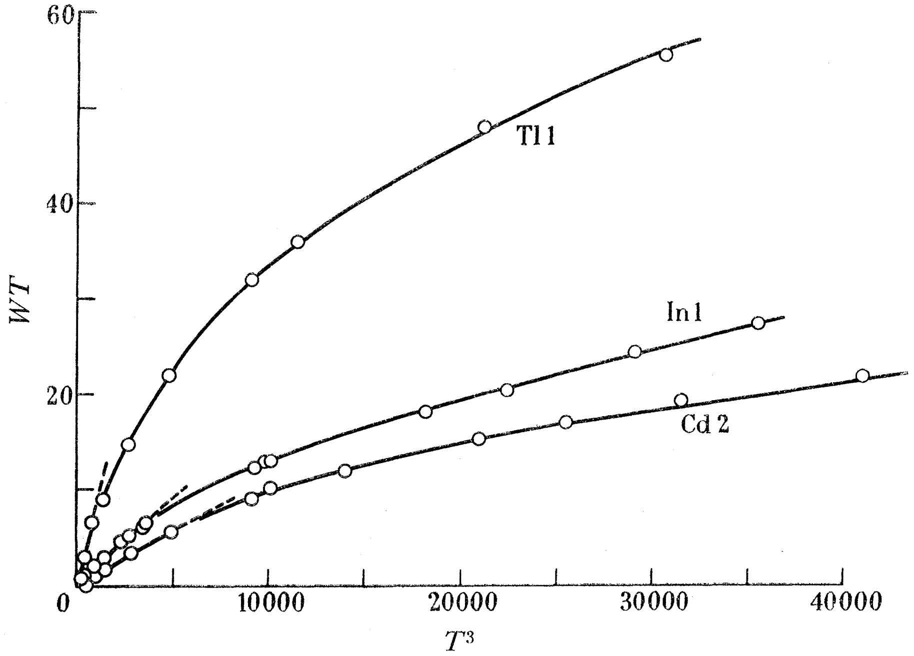

FIGURE 38. Graphs of WT against T^3 for the specimens of thallium, indium and cadmium. These illustrate the bending over of the curves towards the T^3 axis at higher temperatures where the low-temperature approximations are no longer valid.

In this description of the results we have frequently mentioned the curves of WT against T^3, the slope of which determines the coefficient α. From the simple expression for the thermal resistance (equation (9)) these graphs should be linear. In actual fact, however, they are seldom perfectly straight lines, and using the higher approximations of the theory we have previously shown (Olsen & Rosenberg 1953) what departure from linearity should be expected.

If Sondheimer's (1950) results are used, then for an ideally pure metal the WT curve deviates from linearity by 10 % (i.e. the slope is changed by 10 %) at a temperature of approximately 0·125 θ. With increasing impurity this deviation starts at progressively lower temperatures. It was not possible to measure a sufficient range of specimens of one metal with different impurity contents to see if these calculations were correct, but

---

* *Note added in proof* (12 *January* 1955). A recent extension of the work on Cd (unpublished) has, however, shown signs that at the lowest temperatures the $WT \sim T^3$ graph changes to a straight line of steepness 40×10^{-5}. Indication of a similar effect has also been noted in Zn. This would leave the factor $K_\infty \theta^2 \alpha$ still the same for both metals but would bring its numerical value to 11·4.

nevertheless, in many cases the WT curves do show the bending over which is to be expected at higher temperatures and the temperature at which this bending starts is dependent on the value of θ. There would seem to be no advantage in presenting graphs of all these WT curves, but in figure 38 we show those of Cd2, In1 and Tl1. These give an indication of the general behaviour.

The initial section of the WT curves, which should in all cases be linear, is for many specimens not exactly so when examined carefully. Sometimes there is a slight concavity and in others a slight convexity. In the case of Mg2 and Fe1 this has been related to anomalies in the electrical resistance. Other such deviations have already been noted in connexion with the individual metals. The most common behaviour is for the WT curves to start linearly with one slope and then, between 5 and 10° K (depending on the metal), for the curve to become steeper and then to have another linear section with a larger slope. This occurs with Sn1 and Pb1 (see figures 19 and 21) and also with the gallium specimens. This change of slope occurs at a temperature in the neighbourhood of the maximum in the thermal conductivity curve. It is here that the impurity resistance term and the lattice scattering resistance term are of the same order of magnitude. It might therefore be due to the fact that Matthiesen's rule is not strictly valid in this region.

It should not be expected, however, that the theory, which is derived for monovalent metals, although it gives a good qualitative picture of polyvalent metals as well—should hold to the extent of the higher approximations of the $WT \sim T^3$ relationship. For the monovalent metals, copper, silver and gold, the initial sections of the WT curves do seem to be linear.

10. The approximate determination of the thermal conductivity of a given sample of a metal

It sometimes happens that a knowledge of the thermal conductivity of a metal is required in the low-temperature range without a thermal conductivity measurement having to be made. It will have been evident from a study of this paper that a definite figure cannot be given, since at low temperatures the thermal conductivity depends to a large extent on the chemical and physical impurities of the particular sample. If, however, the residual electrical resistance of the specimen is known, then sufficient data are available for an approximate calculation of the thermal conductivity for temperatures up to about $\theta/5$. The determination of the residual electrical resistance, ρ_i, is very simple providing some liquid hydrogen or liquid helium is available. In most cases the electrical resistivity at liquid-hydrogen temperature is the value of ρ_i approximately, but with an extremely pure specimen, or one with a low Debye temperature, it would be advisable to measure the resistivity in a liquid-helium bath. If we use the appropriate value of α from Table 2 we then have from equation (9)

$$1/K = \alpha T^2 + \rho_i/L_0 T = \alpha T^2 + \rho_i/2{\cdot}45 \times 10^{-8} T,$$

and hence K can be calculated for any given temperature, T. This expression should give an answer that is sufficiently accurate for the solution of any technical problem. It should, however, be emphasized that the electrical resistance measurement for ρ_i must be done on a sample whose chemical and physical condition is exactly the same as that of the metal whose thermal conductivity is required. The method might not give good results for very impure metals or for alloys, since there might be some lattice conductivity present. Nevertheless, it should give a lower limit to the conductivity.

I should like to thank Dr K. Mendelssohn, F.R.S., for the great interest that he has shown in this work. I should also like to thank those persons who very kindly provided or prepared some of the specimens. These were Dr A. J. Goss and Mr S. Weintroub, of the University of Southampton, Dr R. W. Powell, of the National Physical Laboratory, The Director, Dr Geach and Dr Churchman, of the Associated Electrical Industries Research Laboratories, Messrs Johnson, Matthey & Co. Ltd, and Dr Raine, of Metropolitan Vickers, Ltd.

References

Andrews, F. A., Webber, R. T. & Spohr, D. A. 1951 *Phys. Rev.* **84**, 994.
Bardeen, J. 1937 *Phys. Rev.* **52**, 688.
Berman, R. 1953 *Advanc. Phys.* **2**, 103.
Berman, R. & MacDonald, D. K. C. 1951 *Proc. Roy. Soc.* A, **209**, 368.
Berman, R. & MacDonald, D. K. C. 1952 *Proc. Roy. Soc.* A, **211**, 122.
Bhatia, A. B. 1949 *Proc. Phys. Soc.* B, **62**, 229.
Bijl, D. & Pullan, H. 1955 (to be published).
Blackman, M. 1951 *Proc. Phys. Soc.* A, **64**, 681.
Boas, W. & Mackenzie, J. K. 1950 *Progr. Metal. Phys.* **2**, 90.
Churchman, A. T. 1953 *Nature, Lond.*, **171**, 706.
Cook, D. B., Zemansky, M. W. & Boorse, H. A. 1950 *Phys. Rev.* **78**, 820.
de Haas, W. J. & Bremmer, H. 1936 *Physica*, **3**, 672.
de Haas, W. J. & de Nobel, J. 1938 *Physica*, **5**, 449.
de Haas, W. J. & Rademakers, A. 1940 *Physica*, **7**, 992.
Grüneisen, E. & Adenstedt, H. 1938 *Ann. Phys., Lpz.*, **31**, 714.
Grüneisen, E. & Erfling, H. D. 1940 *Ann. Phys. Lpz.*, **38**, 399.
Grüneisen, E. & Goens, E. 1932 *Ann. Phys.* **14**, 164.
Hulm, J. K. 1950 *Proc. Roy. Soc.* A, **204**, 98.
James, N. R., Levgold, S. & Spedding, F. H. 1952 *Phys. Rev.* **88**, 1092.
Kemp, W. R. G., Sreedhar, A. K. & White, G. K. 1953 *Proc. Phys. Soc.* A, **66**, 1077.
Klemens, P. G. 1954 *Proc. Phys. Soc.* A, **67**, 194.
Kohler, M. 1949 *Z. Phys.* **125**, 679.
Kroll, W. 1938 *Sci. Pap. Inst. Phys. Chem. Res., Tokyo*, **34**, 194.
MacDonald, D. K. C. 1947 *J. Sci. Instrum.* **24**, 232.
MacDonald, D. K. C. 1952 *Phys. Rev.* **88**, 148.
MacDonald, D. K. C. & Mendelssohn, K. 1950 *Proc. Roy. Soc.* A, **202**, 103.
Makinson, R. E. B. 1938 *Proc. Camb. Phil. Soc.* **34**, 474.
Mendelssohn, K. 1951 *Proc. N.B.S. Low Temp. Symp.* p. 253.
Mendelssohn, K. & Olsen, J. L. 1950*a* *Proc. Phys. Soc.* A, **63**, 2.
Mendelssohn, K. & Olsen, J. L. 1950*b* *Proc. Phys. Soc.* A, **63**, 1182.
Mendelssohn, K. & Olsen, J. L. 1950*c* *Phys. Rev.* **80**, 859.
Mendelssohn, K. & Pontius, R. B. 1937 *Phil. Mag.* **24**, 777.
Mendelssohn, K. & Renton, C. A. 1953 *Phil. Mag.* **44**, 776.
Mendelssohn, K. & Rosenberg, H. M. 1952*a* *Proc. Phys. Soc.* A, **65**, 385.
Mendelssohn, K. & Rosenberg, H. M. 1952*b* *Proc. Phys. Soc.* A, **65**, 388.
Mendelssohn, K. & Rosenberg, H. M. 1953 *Proc. Roy. Soc.* A, **218**, 190.

Olsen, J. L. 1951 D.Phil. Thesis, Oxford University.
Olsen, J. L. 1952 *Proc. Phys. Soc.* A, **65**, 518.
Olsen, J. L. & Renton, C. A. 1952 *Phil. Mag.* **43**, 946.
Olsen, J. L. & Rosenberg, H. M. 1953 *Advanc. Phys.* **2**, 28.
Olsen-Bär, M. & Powell, R. W. 1951 *Proc. Roy. Soc.* A, **209**, 542.
Peierls, R. 1929 *Ann. Phys., Lpz.*, **3**, 1055.
Powell, R. W. 1951 *Proc. Roy. Soc.* A, **209**, 525.
Powell, R. W. 1953 *Phil. Mag.* **44**, 645.
Rosenberg, H. M. 1954*a* *Phil. Mag.* **45**, 73.
Rosenberg, H. M. 1954*b* *Phil. Mag.* **45**, 767.
Sondheimer, E. H. 1950 *Proc. Roy. Soc.* A, **203**, 75.
Sondheimer, E. H. 1952*a* *Proc. Phys. Soc.* A, **65**, 561.
Sondheimer, E. H. 1952*b* *Proc. Phys. Soc.* A, **65**, 562.
Tyler, W. W., Wilson, A. C. & Wolga, G. J. 1952 *Knolls Atomic Power Lab. Rep.* no. 802.
Umeda, K. & Toya, T. 1949 *J. Fac. Sci. Hokkaido Univ.* (2), **3**, 257.
Umeda, K. & Yamamoto, T. 1949 *J. Fac. Sci. Hokkaido Univ.* (2), **3**, 249.
Umeda, K. & Yamamoto, T. 1951 *J. Fac. Sci. Hokkaido Univ.* (2), **4**, 65.
Wert, C. 1950 *Thermodynamics in physical metallurgy*, p. 178. American Society for Metals.
White, G. K. 1953*a* *Proc. Phys. Soc.* A, **66**, 844.
White, G. K. 1953*b* *Proc. Phys. Soc.* A, **66**, 559.
Wilson, A. H. 1937 *Proc. Camb. Phil. Soc.* **33**, 371.
Ziman, J. M. 1954 *Proc. Roy. Soc.* A, **226**, 436.